Relation between soil properties and aggregate stability in the West Usambara Mountains, Tanzania

Lisette Peters

Universiteit Utrecht

Relation between soil properties and aggregate stability in the West Usambara Mountains, Tanzania

MSc Thesis

May, 2019

Author: Lisette Gabrielle Maria Peters

Student number: 4075900

E-mail: l.g.m.peters@students.uu.nl

First supervisor: Geert Sterk

Second supervisor: Juma Wickama

MSc Programme: Earth Surface and Water

Faculty of Geosciences

Department of Physical Geography

Utrecht University

Acknowledgements

This research was supported by the Agricultural Research Institute Mlingano (ARI), in Tanzania. My greatest gratitude goes out to the colleagues who helped me in the lab and in the field, but more importantly, introduced me to the wonderful Tanzanian culture. Michael, Catherine, Lucius and Juma and the locals from Mlingano, assante sana! Furthermore, I would like to thank my supervisor Geert Sterk, who was always available for very helpful advice whether I was in Utrecht or Tanzania.

Abstract

In an earlier erosion study conducted on six fields in the Usambara Mountains, it became apparent that aggregate stability significantly differed between erodible- and non-erodible fields. The dynamics controlling aggregate stability are often difficult to assess since it highly depends on soil specific circumstances. The aim of this research therefore was to determine the relation between aggregate stability, soil organic matter (SOM), soil chemical properties and clay mineralogy. For both erodible- and non-erodible fields water-drop tests were performed to test the aggregate stability. From the same field locations, soil samples were collected for a physicochemical research. The correlation matrix revealed that C, N and CEC are significant positively related to aggregate stability. For wet aggregate stability, this also included the variables P and K. For dry aggregate stability, Fe was significantly correlated. A conclusive correlation for cations and aggregate stability could not be made. Kaolinite was the dominant clay type for all six fields. Kaolinite-dominated soils favor oxide-binding due to low negative surface area. Its clay structure explains the unexpected findings on the cation relations to aggregate stability. In this study, both Fe and SOM turned out to positively influence aggregate stability. The most important variable affecting aggregate stabilities between erodible- and non-erodible fields is SOM. Multi-variate models were composed using multi-linear regressions for both wet-and dry aggregate stability. The most influential soil parameters for both models are C and Fe. The wet aggregate stability models resulted in weak fit, whereas the dry aggregate stability models showed strong predictive capabilities. Dry aggregates were assumed to correspond better to favorable soil composition, which allows for an easier fitted model. A function for aggregate stability in relation to rainfall detachment was implemented into the rMMF model. The extended model functions well with the newly implemented aggregate stability function. By increasing both the EHD and aggregate stability, lower annual erosion values are modelled. The function still resembles rainfall detachment processes, but now incorporates the aggregate stability into the calculations.

Table of contents

1. Introduction

1.1 Background:

The Usambara Mountains in Tanzania are part of the densely populated highlands of Eastern Africa. These highlands mark their agro-socio-ecological importance with its reliable precipitation, fertile soils and well developed vegetation cover (Berry and Turner, 1990). Due to these favorable climatic conditions, the Tanzanian highlands experience a significantly higher crop productivity potential compared to other regions within the country. This has led to high population densities. In 2012 the total population consisted of 492,400 inhabitants thereby illustrating an increase of 1.63% population increase as measured from 2002 onwards. The total Tanzanian population has almost doubled since 1967 with an annual growth rate of 2.9% (Tanzania National Consensus, 2014).

The high population density has led to intensive cultivation and overexploitation of natural resources, which has resulted in severe soil erosion and soil fertility deterioration in the East African highlands (Lundgren & Lundgren, 1979). The intensified soil erosion processes that occur within these highlands are more pronounced due to steep topography and deforestation practices in order to obtain new land (Ezaza, 1988). Consequently, Tanzanian farmers experience a serious constraint to their crop production, as such rates of soil erosion result in sufficient loss of the fertile top soil. The negative effects on agriculture and food security severely enhance the poverty rates in this region, as both food and income are mainly focused on local farming activities (Mahoo et al., 2015)

Soil erosion is a process that involves two phases, where the individual particles are detached from the soil mass by an erosive agent such as wind or rain, which at its turn transports the detached particles. The ease of which particles are detached from the soil is also known as the soil erodibility factor (Renard et al., 1997). An important influence on erodibility is a soil's aggregate stability, as for a higher aggregate stability, a lower soil erodibility exists (Kemper & Rosenau, 1986). This relation is important when dealing with excessive soil losses, since this particular soil property could significantly improve soil erodibility.

The agricultural soils located in the Usambara mountains have similar climatic conditions and slope steepness, but experience different rates of soil erosion. Since there are no major differences between these climate, topography and soil types, erodibility of the soils is likely to cause the differences in soil loss. Earlier research conducted by Gorter (2013) confirmed that the aggregate stability is the main contributor in erodibility differences. It is therefore necessary to determine what causes the differences in aggregate stability for this particular area, in order to adapt current land management operations and lower the soil erodibility.

1.2 Problem definition

An aggregate can be described as a group of particles that are more strongly bound to each other through cohesion than to other surrounding soil particles (Kemper & Rosenau, 1986). The disintegration of soil into aggregates involves the interaction of an erosive force with the soil mass. The aggregate stability is therefore a measure that refers to the ability to withstand disruptive forces acting upon aggregate cohesion. A higher aggregate stability will result in a higher fraction of large pores in the soil. This is beneficial for infiltration rates and aeration for plant growth, which are both important contributors when dealing with excessive erosion rates as runoff and thus erosion is reduced (Jankauskas et al., 2008).

The aggregate stability thus depends on its resistance to disruptive forces, which inhibits the aggregate breakdown. This breakdown may result from four main mechanisms (figure 1), acting upon different scales of soil structures (Le Bissonnais, 1996): 1) slaking, which refers to the compression of entrapped air during rapid wetting; 2) breakdown by differential swelling; 3) breakdown due to kinetic energy of raindrop impact; 4) physicochemical dispersion. The difference between these four mechanisms can be appointed to different kinetics in the processes, differing physical- and chemical conditions required for the disaggregation and differing type of soil properties influencing the mechanism (Farres, 1987; Le Bissonnais, 1988; Römkens et al., 1990; Chan & Mullins, 1994). The different breakdown mechanisms are one of the main differences between the wet- and dry aggregate stability. Dry aggregates experience breakdown by fast wetting (slaking), whereas the wetted aggregates rather experience breakdown by slow wetting (differential swelling).

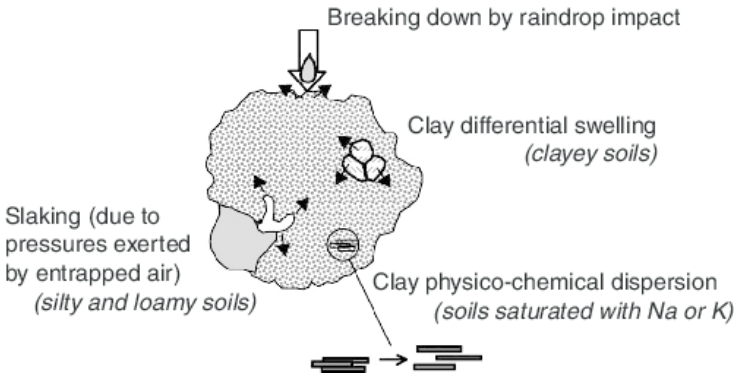

Figure 1: Main aggregate breakdown mechanisms (Chenu and Cosentino, 2011).

The main soil properties that influence aggregate stability frequently have been a topic of soil research interest. In literature, the properties that have been discussed most often include soil texture, clay mineralogy, organic matter content, concentration of cations and $CaCo_3$ content (Le Bissonnais, 1996). Within this range of soil properties, the soil organic matter content (SOM) has been reported numerous times as the most important aggregate stabilizer. It is assumed that SOM increases the cohesion of aggregates through the binding of mineral particles by organic polymers (Tisdall and Oades, 1982; Chenu and Guerif, 1991; Dorioz et al., 1993; Chenu et al., 1994). In 2:1 clay-dominated soils, SOM acts as a major binding agent due to its polyvalent metal-organic matter complexes that interact with negatively charged 2:1 clay particles. Moreover, SOM also decreases the wettability of aggregates through its hydrophobic nature, which results in decreased breakdown by slaking (Sullivan, 1990).

The relation between SOM and aggregate stability is however not as straight forward as often mentioned. Denef and Six (2005) stated that SOM may serve on a different level as an aggregate stabilizer depending on the type of clay mineralogy present in the concerning soils. Clay minerals in the soil can be of great importance, as they control soil chemical properties such as surface area and cation exchange capacity (Dixon and Weed, 1989). The kaolinitic soils were found to rapidly form macro aggregates due to its relatively large 1:1 clay mineral content, which stimulates the electrostatic interactions between the clay minerals and oxides. This type of mineralogy is characteristic for highly weathered soils. Hence, oxide is in this case the dominating aggregate stabilizing agent, rather than SOM. Results from the research performed by Denef and Six (2005) confirmed the difference in the role of SOM for a kaolinitic soil compared to an illitic soil (2:1 clay content), due to a different type of electrostatic interactions between differing clay type contents. It was proven that illitic soils form stronger organic bonds, resulting in a long-term stability of the aggregates when compared to those in kaolinitic soils (Denef and Six, 2005).

Consequently, the mineralogical characteristics of a soil can be of great influence of aggregate stability and the relationship between SOM and aggregate stability (Six et al., 2002). When

researching the differences in aggregate stability, it is therefore important to evaluate both the SOM content in combination with clay mineralogy content as these might affect each other. This has also been claimed by Morgan (2005), who showed that the occurrence of smectite and vermiculite may decrease the stability of aggregates.

There has been much research conducted on the effects of certain soil properties on aggregate stability and resulting erodibility. However, Emerson and Greenland (1990) proposed that the relations that have been found between these parameters may not be applied to all soils in all circumstances. It is therefore important to determine these relations for the soils within the region of interest, and incorporate them into soil erosion models for a more accurate assessment of soil erosion.

When modelling the erosion rates within the Lushoto region, the Morgan-Morgan-Finney model has been applied several times (Gorter, 2013; Wickama, 2010). The MMF Model predicts annual soil loss from field-sized areas on hill slopes. As proposed by Gorter (2013), the model would highly benefit from an optimization by implementing an aggregate stability component. The MMF model has been revised and adapted to fit more detailed erosion processes, and is now termed the revised MMF model (Morgan, 2005). The revised model (rMMF) has recently been optimized by Sterk (2019), as it is now capable of dealing with irregular hill slopes where re-infiltration is allowed. This hillslope version of the rMMF model is therefore better when modelling erosion on the Lushoto hillslopes. By incorporating the aggregate stability into the hillslope rMMF model, a more accurate simulation of erosion rates for the Usambara fields located on the hillslopes can be realized.

The overall aim of this research is to determine the causes for aggregate stability differences in soils of the West Usambara Mountains, and how these differences influence water erosion processes and rates. The following specific objectives have been formulated:

1. Determine the relation between aggregate stability, SOM content, soil chemical properties and clay mineralogy for the Usambara fields.
2. Develop predictive models for wet- and dry aggregate stability
3. Extend the hillslope rMMF erosion model with an aggregate stability parameter to achieve improve simulation of erosion rates in the Usambara Mountains

2. Study area

The research was performed in the vicinity of a village called Soni, Lushoto district located in the West Usambara mountains in Tanzania. The study area is located within the latitudes -4° 05' to -5° 00' and longitudes 38° 50' to 38° 40' (Ezaza, 1992). The population density in 2010 was 120 people per km^2 (Wickama, 2010). The Usambara mountains consists of two Precambrian rock mountain segments belonging to the Usagaran system. The segments are referred to as the West- and East Usambara mountains. Lushoto district is located in the western part of the Usambara Mountains. The district is characterized by a steep, mountainous topography where soils are derived from metamorphic rocks such as gneisses and granulites. Typical minerals occurring in these types of rock are horn-blend-andesine-quartz and diopside-andesine quartz (Geological Survey of Tanganyika, 1963). Long-term erosion cycles have created many sharp mountain ridges stretching from northwest to southeastern direction. A system of permanent streams runs between these ridges, conjoining at the southern outlet (Meliyo et al., 2000).

In the soil analysis performed for Lushoto district by Meliyo et al. (2001), five different mapping units were distinguished. The soils at the summit were classified as 'humic acrisol' and steeper slopes found at the foot of the summit are classified as 'haplic lixisol'. At the ridges and dissected parts the soils were classified as 'haplic acrisol'. The soils located at the river valley were classified as 'eutric fluvisol' and 'umbric gleysol'. The soil profile comprises of multiple soil layers. The topsoil in Lushoto district consists of a thick, dark reddish brown color. The subsoil layers tend to be yellowish red as the organic matter content is declining with increasing depth. Here, small pieces of weathered rock can be found. Texture wise, a high percentage of clay (25-60%) was documented for all Lushoto soils (Mwango et al., 2015). In general, the soils in the Usambara Mountains are considered to be highly weathered (Ndakidemi and Semoka, 2006).

The altitude of the Usambara highlands ranges from 600 to 2300 meters above mean sea level (Pfeiffer, 1990). Daily temperatures range between 18 to 23 degrees Celsius (Wickama and Mowo, 2001). The area is characterized by a bimodal rainfall pattern with a long rainy season between February and May, and a short rainy season from October until December. The total annual rainfall comprises of 400 mm in the lowlands to 1800 mm in the highlands (Mahoo et al., 2015).

Most of the cultivation on the arable lands in the Lushoto region takes place in the valley bottoms, where the most commonly cultivated crops are coffee, tea, various vegetables, maize and bananas (Meliyo et al., 2001). The area began facing a severe rate of land degradation when commercial crops were introduced (Johansson, 2001). Before the introduction of the commercial crops, most lands in the Usambara's were protected by natural forests where traditional agroforestry was practiced (Scheinmann, 1986).

However, natural resources in the area were quickly being over exploited as a great demand rose from the growing population density (Conte, 1999). It led to an increased rate of deforestation and changes in cultivation systems. The traditional agroforestry was replaced by mono-cropping systems, which demanded regular clearings of the farmers plots which induced a higher rate of soil erosion (Woytek et al., 1987).

Currently, soil erosion is occurring throughout the entire Usambara region and thereby forming a major constraint to agricultural production (Tenge et al., 2004). It leads to crop burial, loss of soil nutrients which indirectly induces the deterioration of the structure of soil (Lal, 1985). The amount of top soil erosion in the West Usambara Mountains has been reported up to 100 t ha^{-1} annually (Kaswamila and Tenge, 1998).

For this research, six fields were selected which already have been used in a previous study. Gorter (2013) made an erodibility classification using visible erosion features such as rill-and gully formation. Table 1 gives the main features of these six fields. The erodible soils have a reddish brown color (figure 2), whereas the non-erodible fields appear much darker brown (figure 3). Clay is the dominating soil fraction with small fractions of sand. All six fields are acrisols. There were no differences observed in soil porosity and stones presence between the erodible- and non-erodible sites. Almost all soil profiles contained small pieces of weathered quartz and gneisses. Differences in compaction between the fields can all be appointed to the degree of vegetation present in the soil.

Table 1: Information of the study fields in Lushoto District, West Usambara Mountains, Tanzania

Field	**Erodibility**	**Village**	**Slope**	**Cultivation**	**Land management**	**Fertility treatment**
1	Erodible	Shashui	30˚	Maize, beans	None	Cow manure
2	Erodible	Shashui	26˚	Maize, beans	Terraced, grass stripped	Cow manure
3	Erodible	Shashui	24˚	Maize, various fruit trees	Partially terraced	Cow manure, Urea
4	Non-erodible	Kisiwani	28˚	Maize, beans	None	Urea, DAP [a]
5	Non-erodible	Kisiwani	27˚	Maize, beans	Terraced	Urea, DAP [a]
6	Non-erodible	Kisiwani	29˚	Maize, beans, yam, cassava	None	Unknown

[a] Diammonium phosphate fertilizer

Figure 2: One of the erodible fields (field 1)

Figure 3: One of the non-erodible fields (field 6)

3. Materials and Methods

3.1 Field sampling

In order to conduct the soil analysis, samples from all of the selected six fields were collected from five sampling positions. These sampling places are located on the four corners and the middle of the field. The sampling was done using a small shovel. The samples were taken from the upper soil layer (0 – 5 cm), since this layer contains the maximum spatial variation in organic carbon (Siband, 1974; Mann, 1986; Walker and Desanker, 2004). Also, erosion occurs at the most upper part of the soil layer, hence only the first 0 to 5 cm was selected as sampling depth. Aggregates were collected from the upper layer of the soil and preserved carefully during sampling and transport. For the soil texture analysis, a second sampling range was performed at 15-30 cm depth using core samplers. Furthermore, at the four corners for each field a core sample was taken to determine the bulk density and soil moisture content.

3.2 Soil physical analysis

Before each of the chemical analyses performed on the samples, the soil was grinded and sieved through a 2mm sieve. If the soil was moist from previous rainfall, it was dried on a tray for 3 to 4 days until air-dry.

Soil texture & bulk density

The soil texture was determined according to hydrometer method (Bouyoucos, 1962), where no pretreatments were applied. The percentages clay, fine silt and coarse silt, and sand were determined. The soil texture class was determined using the soil texture triangle (figure 4). The texture was analyzed at 0 – 15 cm depth and at 15-30 cm depth to observe any potential changes within the soil layers.

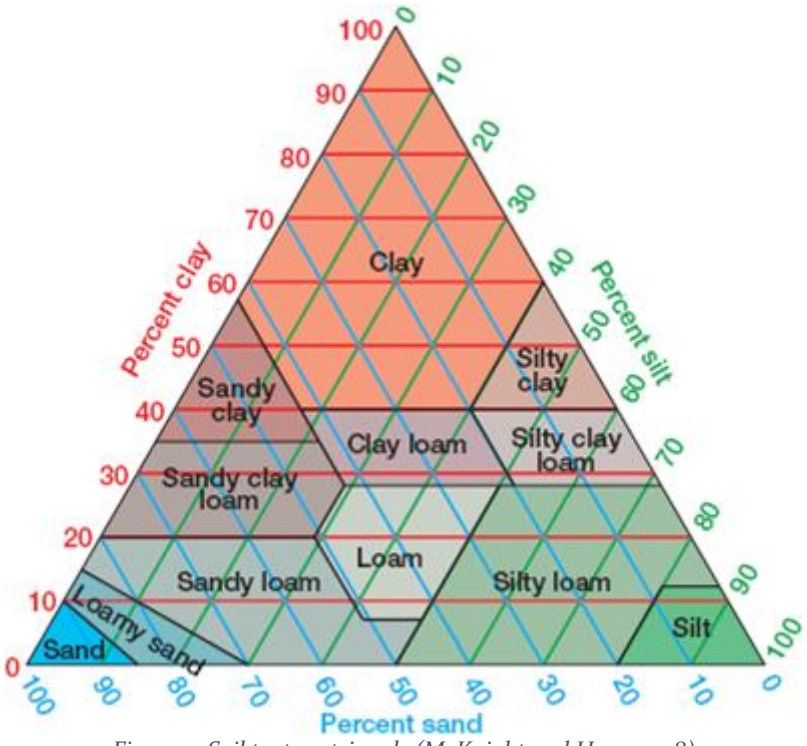

Figure 4: Soil texture triangle (McKnight and Hess, 2008)

Aggregate stability

In the paper published by Imeson and Vis (1984), a simple yet rapid method is described to measure the wet- and dry aggregate stability. Imeson and Vis (1984) chose the CND (Count Number Drops) method due to its simplicity and its accessibility on a wide variety of samples. The CND test has been widely adopted and performed in several other studies on aggregate stability (Lavee and Sarah, 1995; Cerda, 1998). The water drop test method as proposed by Imeson and Vis (1984) was therefore selected for this research. A similar construction as described by Imeson and Vis (1984) was built, along with a digital drop counter incorporated into the system to ease the process and limit the measurement errors.

The dry aggregates were sieved until the 4.0 – 4.8 mm fraction was obtained. The aggregates were then placed under a 1 m high pipe with a 15 cm diameter, where the aggregates were struck at a constant pace with equally sized water drops. The number of drops was recorded until the aggregate was defragmented to a size of 2.8 mm. This moment was observed visually when the fragments would pass through the 2.8 mm sieve on which the aggregate was positioned. The number of drops required for breakdown provided an index of aggregate stability. For measuring the wet aggregate stability, the samples were pre-moistened at pF = 2.0 with distilled water, 24 hours prior to the measuring moment. Soil moisture measurements indicated the amount of water required to reach this pF level.

Before each new aggregate was placed on the sieve, the surface was made dry in order to avoid pre-wetting of the aggregate. This method was repeated for five dry- and wet aggregates from five different locations in one field. These locations consist of the four corners and the middle of the field. This comprised 50 aggregate stability measurements for each field of the total six fields.

The aggregate stability indices were converted into kinetic energy values. The CND test device was set at a constant drop size of 0.1 grams. The falling velocity of a single water drop was derived from a numerical model that simulates the falling velocity of rain drops and is assumed equal to 1.4 m/s (van Boxel, 1997). The total kinetic energy of a water drop after 1-meter distance was multiplied to the number of required drops per aggregate breakdown.

Soil chemical analyses

For all analyses performed, 5 samples per field were used. These are from the identical locations of the aggregate stability measurements. The content of soil organic carbon of the field samples was determined by using the wet combustion Walkley-Black (1934) chromic acid wed oxidation method. The total nitrogen content analysis was performed according to the semi-micro Kjedahl method (Kjedahl, 1983). The total available phosphorus content was determined according to the method of Bray and Kurtz (1945).

Exchangeable sodium (Na), potassium (K), calcium (Ca) , and magnesium (Mg) were determined directly in a 1.0 M neutral ammonium acetate filtrate. From this solution, the amounts of sodium and potassium were flame-photometrically determined, while calcium and magnesium measures were obtained using atomic absorption spectrophotometry (Chapman, 1965). The cation exchange capacity (CEC) was determined according to the ammonium acetate method at pH=7.0. The pH was determined in a soil-water dispersion of 1:2,5 where the sample was shaken for 30 minutes and directly read from the pH meter.

A dry analysis was performed using a spectrometer, where trace elements Fe and Al were determined based on alpha particle spectroscopy. The samples were finely grounded to obtain a powder texture before placement into small container that entered the machine. Obtained

wavelengths were translated into trace elements with corresponding quantities present in the sample.

Clay mineralogy

As proposed by Mansu (2006), X-ray powder diffraction (XRD) serves as the most efficient method when dealing with clay minerals. Each mineral has its own unique inter-reticular spaces, which enables an identification of minerals from the sample (Dutrow, 1997).

For this study, an XRD-analysis was performed using a Bruker-AXS D8 advance powder X-ray diffractometer. In this analysis, five samples from the erodible fields and five samples from the non-erodible fields were used. For each field, one sample was taken from the center location of the field. Additionally, two extra samples for one erodible- and one non-erodible field from the upper corners were analyzed. Evaluating extra samples allowed for a better confirmation on the clay mineral identification.

The samples were finely grinded with a mortar to obtain a powder texture. For each sample, a glass plate with around 1 gram of soil was prepared, where much care was taken in the process to avoid the disturbance of random orientation of the clay minerals (Zhou et al., 2018). The samples were placed into the diffractometer, where each sample was individually measured. The results were compared to a clay mineralogy database in order to identify the samples based on their measured diffracted peaks (d-spacings).

3.4 Statistical analysis

A statistical analysis was performed in Excel using F-tests, to test for significant differences between variances for the erodible- and non-erodible sites. Depending on the outcome, a t-test for equal- or unequal variances was performed to test significant differences for the mean values of the erodible- and non-erodible sites. Specific soil properties were tested at a 90% confidence level (α=0.10). A correlation matrix was made for the chemical variables to aggregate stabilities that consists of correlation coefficients ranging between -1 and 1.

These correlations were tested for their significance using single linear regressions. Additionally, two multi-linear regression analyses were performed for both wet- and dry aggregate stability. These analyses were used to determine the most relevant soil chemical properties in relation to aggregate stability. From these variables, two multivariate models were derived. The predictive abilities of the obtained multi-variate models were tested against the actual measured values. All statistical analyses are incorporated in appendix A and B.

3.5 Extension of the rMMF model

The revised Morgan-Morgan-Finney model is an empirical annual erosion model created for tropical conditions (Morgan, 2001). The model separates the water erosion dynamics in a water- and sediment phase. The following equations describe the calculations of annual soil erosion at field scale (Morgan, 2001; Morgan, 2005).

The calculation of the rainfall kinetic energy (KE; J/m²) is based upon the effective rainfall (P_e; mm). This parameter is the fraction of annual rainfall P not being intercepted by the vegetation canopy (A; fraction between 0 and 1):

$$P_e = P(1 - A) \quad (1)$$

P_e is divided into direct through fall (DT; mm) and into leaf drainage (LD; mm). The leaf drainage is a function of the canopy cover (CC);

$$LD = P_e CC \quad (2)$$

Where the remaining part of P_e is therefore the direct through fall (DT):

$$DT = P_e - LD \quad (3)$$

The kinetic energy is calculated for both LD and DT. For KE(DT) (J/m²), the rainfall intensity (I mm/h) is used in the calculation. This variable is specific for each climatic region (Morgan, 2001). The relation between the kinetic energy and intensity varies as drop-size distribution of the rainfall differs for different geographical regions. As suggested by Hudson (1965), the following KE(DT) equation applies to tropical climatic regions:

$$\mathrm{KE(DT)} = 29.8 - (127.5 / \mathrm{I}) \quad (4)$$

The KE(LD) is a function based upon plant canopy height (PH; m). The following equation is used, as proposed by Brandt (1990):

$$KE(LD) = [(15.80PH^{0.5}) - 5.875]LD \quad (5)$$

The total rainfall kinetic energy thus becomes:

$$KE = KE(DT) + KE(LD) \quad (6)$$

The annual surface runoff (SR; mm) is calculated as follows:

$$SR = P \exp(-\frac{S_c}{P_o}) \quad (7)$$

Where S_c is the soil moisture storage capacity (mm) and P_o the average rain per rainy day (mm), with S_c being described as:

$$S_c = 1000\ MS\ BD\ EHD\ (\frac{Et}{Eo})^{0.5} \quad (8)$$

With MS being the gravimetric soil moisture content at field capacity (kg/kg), BD the dry bulk density of the soil (mg/m³), EHD the effective hydrological depth of the soil (m) and Et/Eo the ratio of actual- and maximum crop evapotranspiration respectively.

Soil particle detachment induced by raindrops (F; kg/m²) is described by the following equation:

$$F = 10^{-3} K\ KE \quad (9)$$

With K as the soil detachability index (g/J), also known as the detachability factor.

Soil particle detachment induced by runoff (H; kg/m²) is described as follows:

$$H = 10^{-3}(0.5COH)^{-1} SR^{1.5} sin(S)(1 - GC) \quad (10)$$

Where COH is the cohesion of the soil surface (kPa), S is the slope (°) and GC the fraction of ground covered with vegetation (0-1).

The transport capacity of surface runoff controls the limitation of the of total amount of the detached sediment to be transported. This parameter TC (kg/m²) incorporates the crop cover C: (0-1) and is calculated as:

$$TC = 10^{-3} C\ SR^2\ sin(S) \quad (11)$$

The final outcome of the rMMF model is the annual erosion rate E (kg/m²), which is expressed by the following equation:

$$E = \min[(F + H), TC] \quad (12)$$

The rMMF model has recently been optimized by Sterk (2019) with a new calculation scheme in order to fit a natural hillslope with irregularities. This hillslope version of the rMMF model is more appropriate for the Lushoto fields and will therefore be used in this research. The following adaptions were implemented by Sterk (2019) to account for the hillslope irregularity:

Hillslope

For the hillslope, sections of i = 1,..,n were made with variable lengths and slope steepness. The top of the hillslope represents the first section, whereas *n* is the lowest section of the slope. For each section, soil- and vegetation characteristics are specified.

Surface runoff

The surface runoff generated for the first slope section (SR_1) is calculated by multiplying SR with the slope length (L_1) and converting the amount in mm to volume per meter:

$$SR'_1 = 10^{-3} SR_1 L_1 \quad (13)$$

Where SR'_1 is in m^2. The second section incorporates the incoming flow from the direct upper section;

$$SR'_2 = 10^{-3} SR_2 L_2 + SR_1 \quad (14)$$

From which a general equation can be derived which incorporates all sections of i = 1,..,n:

$$SR'_i = 10^{-3} SR_i L_i + SR'_{i-1} \quad (15)$$

Re-infiltration

The new rMMF model allows for re-infiltration by introducing the variable LOSS. This variable represents the fraction (0-1) of SR re-infiltrating in a slope section;

$$SR"_i = (SR'_i + SR''_{i-1})(1 - LOSS_i) \quad (16)$$

Sediment transport

The annual detachment H (kg m^2) by overland flow is calculated as follows:

$$H'_i = (0.5 COH_i)^{-1} (SR"_i)^{1.5} S'_i \, (1 - GC) \quad (17)$$

Where COH = cohesion of the soil surface (kPa), S'_i = slope gradient (m m^{-1}), GC= fraction of vegetation cover (0-1). The annual transport capacity becomes:

$$TC'_i = C_i (SR"_i)^{\beta} S'_i \quad (18)$$

With TC'_i in kg m^{-1}, and β a coefficient that can be used to calibrate the model in case of availability of quantitative data.

In the new rMMf model, the calculation of soil loss is accounted for according to the following calculation section:

The sediment transport deficit $ST^{def}{}_i$ in (kg m^{-1}) is calculated by withdrawing the incoming sediment transport from the section above:

$$ST^{def}{}_i = TC'_i - ST_{i-1} \quad (19)$$

The $ST^{def}{}_i$ controls whether deposition of transport occurs, according to the following rules:

- $ST^{def}{}_i$ < 0 results in deposition in the section
- $ST^{def}{}_i$ = 0 results in transport only; no loss or deposition
- $ST^{def}{}_i$ >0, ST depends on the total detachment of the section
    - If $(F_i + H_i')\ L_i \geq TC'_i$ » $ST_i = TC'_i$
    - If $(F_i + H_i')\ L_i < TC'_i$ » $ST_i = TC'_{i-1} + (F_i + H'_i)\ Li$

So far, the hillslope rMMF model does not contain an aggregate stability component. In order to deal with differences in soil cohesion due to deviating aggregate stabilities, a relation with this parameter linked to soil detachment needs to be implemented. In the Limburg Erosion Soil Model (LISEM) by de Roo et al., (1994), a relation has been established between aggregate stability, kinetic energy by rainfall and a corresponding rate of splash detachment:

$$DETR = \left[\frac{2.07}{AGGRSTAB} * KE * exp^{-1.48*depth} + 2.20\right] * (P - I) * \frac{(dx)^2}{dt} \quad (20)$$

Where DETR is the splash detachment (g s^{-1}), AGGRSTAB is the soil aggregate stability (median number of drops), KE = the rainfall kinetic energy (J m^2), depth = the depth of the surface water layer (mm), P = the rainfall (mm), I = the interception (mm), dx is the size of an element (m) and dt = the time increment (s).

The LISEM model is however based on single rainfall events, whereas the rMMF model calculates annual erosion rates. When implementing the LISEM aggregate stability function, an additional conversion was needed to fit into the annual rMMF model. Converting this relation for the annual outcome has been done by using annual values for rainfall for P and KE. Finally, a unit correction was performed to obtain outcomes in m^2:

$$DETR = \left[\frac{2.07}{AGG.STAB} * KE * exp^{-1.48*depth} + 2.20\right] * (P - I) * 10^{-3} \quad (21)$$

The new detachment function is incorporated into the hillslope rMMF model by replacing the initial calculation section of rain drop detachment with the splash detachment equation from the LISEM model. By altering this section in the hillslope rMMF model, the detachability factor K is replaced by the AGG.STAB function.

The following input parameters were used in the adapted rMMF model:

Annual rainfall (R; mm/y)

Hourly rainfall data was collected from an automatic weather station that was installed at a test site in Shashui during the research period of Gorter (2013).

Proportion of the rainfall intercepted by the vegetation or crop cover (A)

The proportion of intercepted rainfall was determined by estimating the main vegetation cover (A; fraction between 0 and 1) on the fields. Typical values for plant species parameters were used as suggested by Morgan et al., (1982).

Proportion canopy cover (CC), proportion ground cover (PC) and plant height (PH; m)

The land cover parameters were determined from estimations made in the field, and expressed as a fraction between 0 and 1.

Crop cover management factor (C)

This factor is the product of the C and P factor from the Universal Soil Loss Equation (USLE) (Wischmeier and Smith, 1978). An estimation for this factor was made according to C values suggested by Morgan et al., (1982).

Typical value for intensity of erodible rain (I; mm/h)

There were no measurements performed on the rainfall intensity, so the intensity was set at 25 mm/h. This is a typical intensity that occurs in tropical climate zones (Morgan, 2005).

Soil moisture content at field capacity (MS; wt%)

The soil moisture content at field capacity (pF=2.0) was measured by taking core samples and performing the pressure cell methodology (Dane & Hopman, 2002). This was done for four locations (0-15 cm) on the corners of the fields. The average from these values was used as input for each field.

Effective hydrological depth of the soil (EHD; m)

The values used for the effective hydrological depth of the soil (EHD) were derived from the recommendations made by Morgan (2001). Here, a crusted bare soil has an estimated EHD of 0.05, whereas a non-crusted bare soil has an estimated EHD of 0.09. Therefore, the EHD value is increased according to this range in order to demonstrate the effects of a higher aggregate stability e.g. difference in erodibility.

Ratio of actual (Et) to potential (Eo) evapotranspiration

The ratio of actual- to potential evapotranspiration used for the model was also derived from values determined by Morgan et al., (1982), where the ratio of Et to Eo depends on the main vegetation cover in the field. When the occurring vegetation type was not included in this table, a similar plant species was selected as equal.

Depth (SL; mm)

This is the depth of the surface water layer (mm). This variable was kept constant at 1 mm, as no information was available to determine this exact value.

Model run scenarios

The model has been run for a steep irregular sloping field, where all of the input parameters were set according to the conditions of field 1 (table 3). This field has a steep, s-curved shaped slope (22-28°) and classified as erodible. The β-value was set at 1.5, since no sediment transport data was available (Prosser and Rustomji, 2000). For each new scenario run, the aggregate stability (AGG.STAB) and effective hydrological depth (EHD) were altered. Table 2 contains an overview of these parameter values implemented for each new model run.

By increasing the effective hydrological depth with increasing aggregate stability, the model accounts for the decreasing rate of crust formation on the soil. Breakdown of aggregates causes the smaller particles to form a crust on the soil that inhibits infiltration, thereby increasing surface runoff and consequent erosion (Le Bissonnais and Arrouays, 1997). By implementing

these changes in the different scenarios, the effect of stronger aggregate stability and related effective hydrological depth on the annual soil erosion in the Lushoto district were simulated.

Table 2: Variable model parameters per model run scenario

Scenario	Agg.Stab (drops)	EHD (m)
1	10	0.05
2	20	0.06
3	30	0.07
4	40	0.08
5	50	0.09
6	60	0.1
7	70	0.11

Table 3: Input parameters for the updated rMMF model for the Lushoto district, Usambara Mountains, Tanzania

Average rainfall:			1050	mm																
Number of raindays:			90	days																
	slope	slope		slope																
Section	length	angle	angle	cum length	Soil	Land use	A	CC	I	PH	MS	BD	EHD	Et/Eo	K	COH	GC	C	LOSS	AGG.STAB	SL
	m	degree	m/m	m			-	-	mm h^{-1}	m	g g^{-1}	Mg m^{-3}	m	-	g J^{-1}	kPa	-	-			
1	3,00	28,00	0,53	3,00	Clay loam	Bare soil	0,00	0,20	25	0	0,4	1,3	0,11	0,40	0,15	100	0,00	0,10	0,00	70,00	1,00
2	3,00	28,00	0,53	6,00	Clay loam	Bare soil	0,00	0,20	25	0	0,4	1,3	0,11	0,40	0,15	100	0,00	0,10	0,00	70,00	1,00
3	3,00	22,00	0,40	9,00	Clay loam	Bare soil	0,00	0,20	25	0	0,4	1,3	0,11	0,40	0,15	100	0,00	0,10	0,00	70,00	1,00
4	3,00	22,00	0,40	12,00	Clay loam	Bare soil	0,00	0,20	25	0	0,4	1,3	0,11	0,40	0,15	100	0,00	0,10	0,00	70,00	1,00
5	3,00	28,00	0,53	15,00	Clay loam	Bare soil	0,00	0,20	25	0	0,4	1,3	0,11	0,40	0,15	100	0,00	0,10	0,00	70,00	1,00
6	3,00	28,00	0,53	18,00	Clay loam	Bare soil	0,00	0,20	25	0	0,4	1,3	0,11	0,40	0,15	100	0,00	0,10	0,00	70,00	1,00
7	3,00	22,00	0,40	21,00	Clay loam	Bare soil	0,00	0,20	25	0	0,4	1,3	0,11	0,40	0,15	100	0,00	0,10	0,00	70,00	1,00
8	3,00	22,00	0,40	24,00	Clay loam	Bare soil	0,00	0,20	25	0	0,4	1,3	0,11	0,40	0,15	100	0,00	0,10	0,00	70,00	1,00
9	3,00	28,00	0,53	27,00	Clay loam	Bare soil	0,00	0,20	25	0	0,4	1,3	0,11	0,40	0,15	100	0,00	0,10	0,00	70,00	1,00
10	3,00	28,00	0,53	30,00	Clay loam	Bare soil	0,00	0,20	25	0	0,4	1,3	0,11	0,40	0,15	100	0,00	0,10	0,00	70,00	1,00

4. Results

4.1 Soil physical properties

Soil texture & Bulk density

For each field, the bulk density was determined at four different locations (figure 5). The distinction between erodibility for the six fields was made with two different colors in the graphs. Most of the obtained bulk density values vary between 1.00-1.40 g/cm³. This range is in accordance with tropical soil bulk densities that are often between 1.00-1.50 kg/cm³ (Zonn, 1986). No significant differences ($\alpha<0.1$) between the average bulk densities of erodible and non-erodible fields were obtained. This result is not in line with other studies performed on this relation, which suggest a lower bulk density as the soil has a higher organic matter content (Dalal and Mayer, 1986).

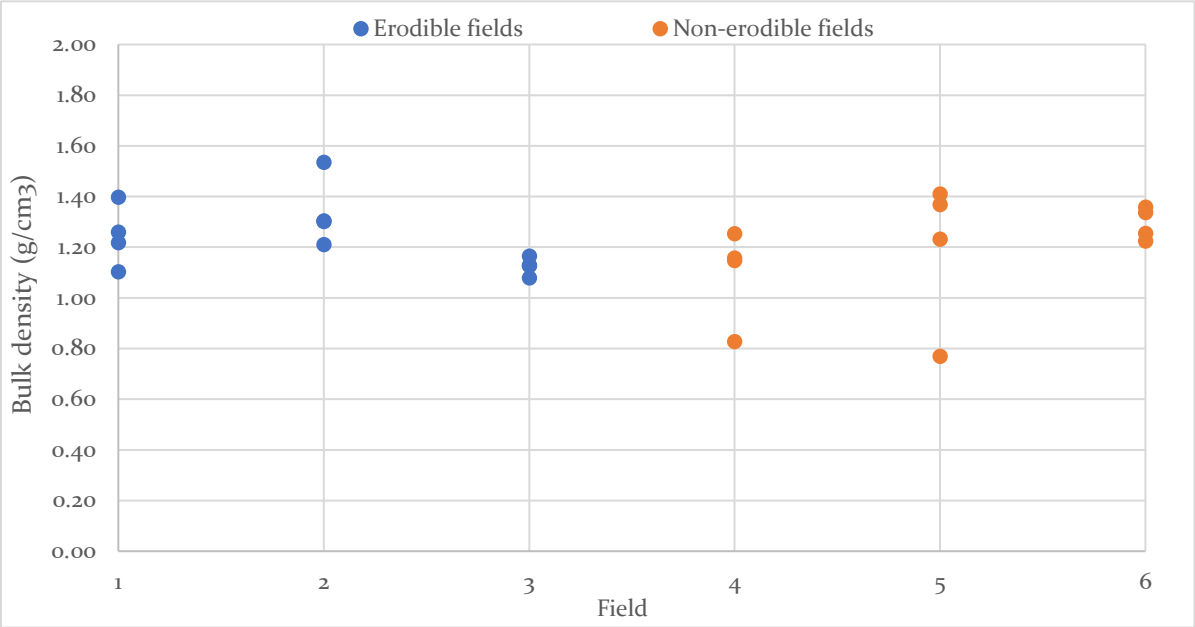

Figure 5: Bulk density values per field

For each of the six fields, the soil texture was determined at two soil depths to observe potential differences in its profile. The results with corresponding texture class are summarized in table 4. The dominant soil texture for all of the fields is clay, followed by some higher sand percentages for especially field 2 and field 5. No significant differences ($\alpha<0.1$) were observed between the six fields for both depth layers. The same is true for the silt and sand percentages. Finally, no significant differences were obtained for clay percentages in the upper and lower layers. In general, all of the six fields are abundant in its clay percentages with substantial sand percentages present. Variations between the texture results are too small to obtain statistically relevant differences for erodible- and non-erodibility.

Table 4: Soil texture analysis per field

Field	%sand	%c.silt	%f.silt	%clay	Texture
1					
0-15 cm	32	4	8	56	Clay
15-30 cm	31	4	7	58	Clay
2					
0-15 cm	41	6	11	43	Sandy clay
15-30 cm	37	5	10	49	Sandy clay
3					
0-15 cm	22	4	14	60	Clay
15-30 cm	24	4	14	58	Clay
4					
0-15 cm	34	6	10	50	Clay
15-30 cm	36	6	10	48	Sandy clay
5					
0-15 cm	40	4	8	48	Sandy clay
15-30 cm	36	4	8	52	Clay
6					
0-15 cm	34	2	8	56	Clay
15-30 cm	30	4	12	54	Clay

Aggregate stability

The aggregate stability measurements are shown in figure 6 (dry aggregate stability) and figure 7 (wet aggregate stability). Each dot represents an average value at one location in the field. The average dry aggregate stability for the erodible fields was 7.6 J and significantly ($\alpha<0.1$) lower than the dry aggregate stability of the non-erodible fields, which have a mean value of 14.0 J. The individual measurements for the erodible fields range between ~4-13 J, whereas for the non-erodible fields this varies between ~8-22 J. For the wet aggregate stability, the average value for the erodible fields was 4.2 J and significantly ($\alpha<0.1$) lower than the average value for the non-erodible fields, which have a mean value of 10.1 J. In general, the wet aggregate stability varies between ~2–7 J for the erodible fields and between ~5-18 J for the non-erodible fields. The stability of the wet aggregates appears to be more inconsistent for the non-erodible fields as these are marked by some high outliers in the measurements. These outliers are caused by the presence of extremely strong aggregates that withstood the threshold of 200 drops (42 J).

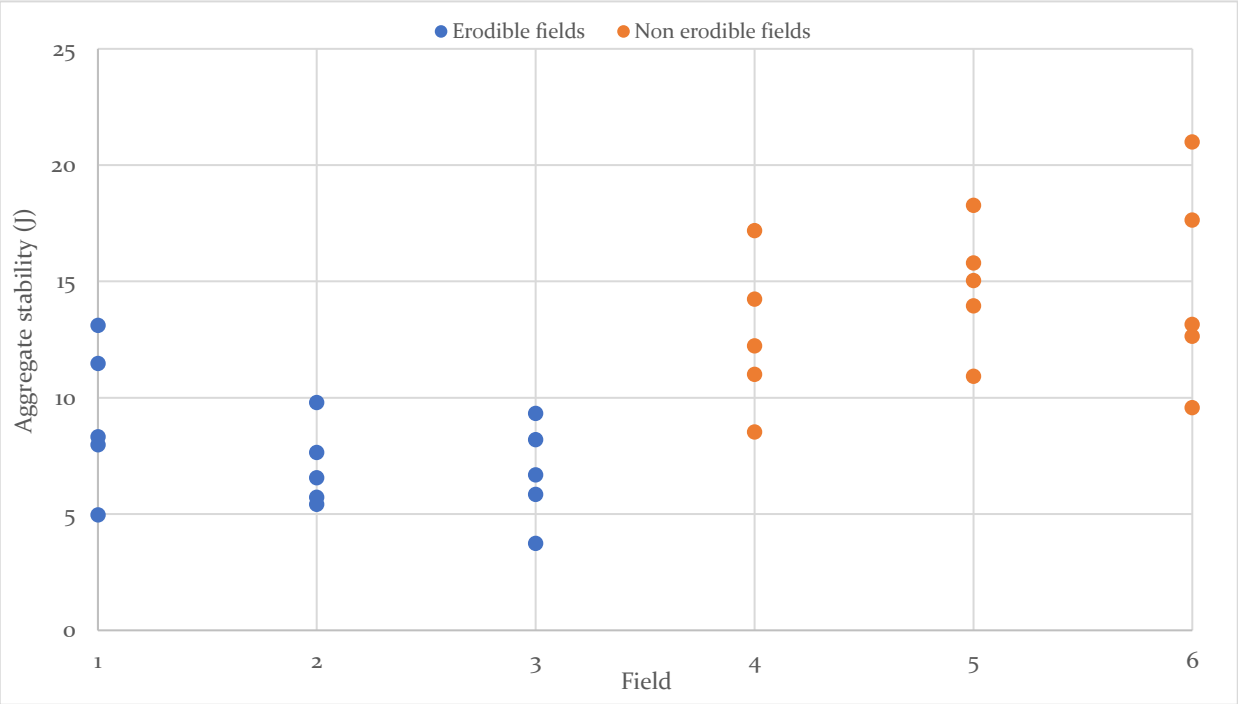

Figure 6: Dry aggregate stability indices per field

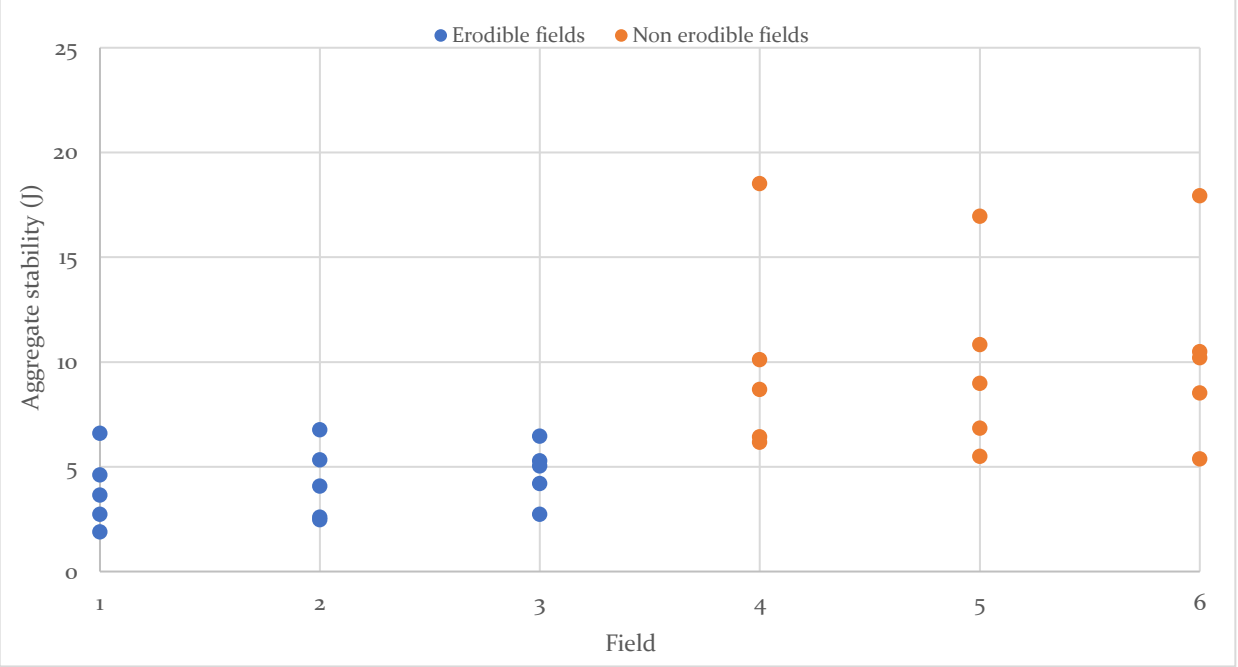

Figure 7: Wet aggregate stability indices per field

4.2 Soil chemical properties

Chemical analyses

All of the results from the chemical analyses performed on the 40 samples in total are summarized table 5. The soil organic carbon percentages of the erodible fields (1- 3) are significantly ($\alpha<0.1$) lower than those of the non-erodible fields (4-6). This corresponds with the first fields interpretations, where the non-erodible classified fields appeared much darker in color due to higher organic matter contents. The C values ranged between 1.49 – 8.1%, which is similar to other soil fertility studies performed in the Lushoto district (Meliyo et al., 2001).

Table 5: Soil chemical analyses of six fields in the Lushoto district, Tanzania

Field	Location	%C	P (mg/kg)	N %	K (cmol+/kg)	Ca (cmol+/kg)	Mg (cmol+/kg)	Na (cmol+/kg)	CEC (cmol+/kg)	Al (mg/kg)	Fe (mg/kg)
1	M[a]	1.49	4.60	0.025	0.057	2.61	0.44	0.023	6.8	28.16	48.03
	1[b]	2.30	6.83	0.023	0.131	55.89	0.69	0.023	7.2	33.06	37.67
	2[c]	1.73	3.95	0.022	0.033	54.89	0.63	0.011	5.8	43.82	32.19
	3[d]	0.74	6.34	0.011	0.016	2.39	0.38	0.011	7.1	31.85	33.76
	4[e]	1.46	1.85	0.022	0.051	2.01	0.23	0.017	6.0	44.14	35.62
	Mean	*1.54*	*4.71*	*0.021*	*0.058*	*23.56*	*0.47*	*0.017*	*6.6*	*36.20*	*37.45*
2	M	2.27	28.73	0.027	0.131	38.92	0.08	0.017	5.7	42.24	20.72
	1	1.60	24.81	0.021	0.117	11.98	3.88	0.011	5.7	35.57	41.41
	2	2.78	3.47	0.033	0.083	6.99	1.25	0.017	8.8	45.16	42.79
	3	2.75	21.53	0.029	0.191	9.58	2.07	0.011	10.0	49.97	39.51
	4	2.18	4.94	0.030	0.070	11.68	1.56	0.017	7.8	61.42	39.54
	Mean	*2.32*	*16.69*	*0.028*	*0.118*	*15.83*	*1.77*	*0.014*	*7.6*	*46.87*	*36.79*
3	M	3.52	1.0	0.029	0.665	8.58	0.84	0.013	6.4	83.25	31.11
	1	3.13	10.7	0.029	4.962	0.10	4.36	0.013	4.4	46.38	27.03
	2	5.79	25.4	0.052	0.665	14.37	1.88	0.020	7.5	21.38	22.00
	3	4.34	9.0	0.037	0.358	9.58	1.91	0.013	5.1	40.19	33.40
	4	3.89	10.7	0.033	0.307	14.17	1.40	0.013	5.6	98.06	27.52
	Mean	*4.14*	*11.3*	*0.036*	*1.39*	*9.36*	*2.08*	*0.014*	*5.8*	*57.85*	*28.21*
4	M	4.68	14.0	0.040	5.575	26.65	2.81	0.013	8.6	51.90	31.29
	1	2.93	-0.1	0.030	1.381	30.44	0.58	0.013	9.7	37.77	43.44
	2	3.40	9.4	0.027	0.972	7.09	1.10	0.027	7.1	85.99	21.33
	3	3.98	15.4	0.030	0.870	14.87	1.79	0.013	10.5	41.71	38.90
	4	6.22	9.1	0.042	0.409	23.15	2.42	0.020	10.7	71.10	42.93
	Mean	*4.24*	*9.6*	*0.034*	*1.84*	*20.44*	*1.74*	*0.017*	*9.3*	*57.70*	*35.58*
5	M	3.29	11.8	0.032	0.665	13.37	3.69	0.013	7.9	47.08	50.48
	1	3.94	12.8	0.043	0.665	36.53	2.07	0.006	7.9	46.38	46.75
	2	5.99	3.1	0.041	1.483	18.66	1.74	0.006	10.3	24.10	27.44
	3	6.33	10.9	0.053	0.716	17.47	1.61	0.027	12.3	52.13	36.84
	4	7.10	10.4	0.043	0.767	15.87	1.42	0.013	10.5	61.89	28.49
	Mean	*5.33*	*9.80*	*0.042*	*0.86*	*20.38*	*2.11*	*0.013*	*9.8*	*46.32*	*38.00*
6	M	3.96	14.0	0.033	2.506	16.67	1.58	0.020	8.1	62.05	39.56
	1	5.41	221.9	0.050	0.512	40.72	1.68	0.034	11.2	47.55	41.13
	2	7.37	130.8	0.053	7.621	14.17	2.86	0.027	9.9	66.57	30.66
	3	4.44	10.7	0.048	2.302	22.26	1.27	0.020	10.4	93.12	30.08
	4	8.09	13.6	0.062	4.041	10.18	2.70	0.034	11.1	25.13	39.53
	Mean	*5.85*	*78.20*	*0.050*	*3.40*	*20.80*	*2.02*	*0.027*	*10.2*	*58.88*	*36.19*

[a] middle ; [b] upper right corner; [c] upper left corner; [d] lower right corer; [e] lower left corner

The average available P values for the six fields ranged between 4.71-78.20 (mg/kg). According to the FMANR (1990), sufficient P levels are 15.0 mg/kg, meaning that especially field 1 and field 3 have below optimal P levels. The erodible fields have significantly lower ($\alpha<0.1$) P values than to the non-erodible fields.

The average N ranges between 0.011- 0.062 %, indicating an overall low amount of total nitrogen in the soils when compared to the fertility survey conducted in the Lushoto district by Wickama and Mowo (2001). The erodible fields have significantly lower ($\alpha<0.1$) N values than the non-erodible fields.

Average exchangeable K ranges between 0.06 – 3.40 cmol/kg, with some unusually high outliers when reviewing the entire soil analysis. Here, the K-values are significantly higher for the non-erodible fields ($\alpha<0.1$). In general, a recommended K value is set at 0.30 cmol/kg (Anderson, (1973). The measured K values are within the same range as found by Meliyo et al. (2001).

Average Mg and Ca values ranges from 0.47 – 2.84 cmol/kg and 9.36 – 23.56 cmol/kg respectively. Both of these exchangeable cation values are consistent with other findings from fertility surveys performed in Lushoto district (Ndakidemi and Semoka, 2006). Measured Ca values do not significantly differ between the erodible- and non-erodible fields ($\alpha<0.1$), where on the contrary the Mg values are significantly higher for the non-erodible fields.

Exchangeable Na varies between 0.011-0.34 cmol/kg, which is slightly lower than the results from the survey by Mwango et al. (2006). The erodible fields have significantly ($\alpha<0.1$) lower average Na values than the non-erodible fields. Generally, the measured Na values for the six fields are low.

CEC values range between 4.4 – 11.1 cmol/kg which is similar to results from Ndakidemi and Semoka (2006). This range of CEC is generally categorized as low (Baize, 1993). The CEC values for the erodible fields are significantly lower ($\alpha<0.1$) than those of the non-erodible fields. For both Fe and Al, no significant ($\alpha<0.1$) differences between the two types of fields were observed.

EC and pH

For all six fields, electrical conductivity and pH values were measured from the sample taken at the center location of each field. The results are illustrated in table 6. In general, pH values measured in the Lushoto area are low (pH <7), but a slight variation between the different erodible sites is observed. The pH of the erodible fields was found to be significantly ($\alpha<0.1$) lower than those of the non-erodible fields. No significant differences were found for the EC values between the two types of fields.

Table 6: pH and EC values of the six fields

Fields	*pH*	*EC (S/m)*
1	4.7	0.01
2	4.7	0.01
3	5.1	0.01
4	5.2	0.01
5	5.3	0.01
6	5.1	0.02

Aggregate stability and soil characteristics

A correlation matrix (table 7) was made based on the total measured aggregate stabilities for the six fields and to the measured chemical variables. The correlation coefficients with an asterisk mark a significant relation (α=0.1). The intensity of the color in the matrix indicates the strength of the correlation between the particular variables.

It becomes evident that much stronger correlations exist for the dry aggregate stability. Here, C, N, Na, CEC and Fe are positively correlated with dry aggregate stability. The strongest correlations exist for dry aggregate stability with N (r=0.59) and CEC (r=0.66). As for the wet aggregate stability, five significant correlations exist. The wet aggregate stability is positively correlated with K, C, P, N and CEC.

Overall, C, N and CEC are positively correlated for both stabilities. No significant correlations were found for variables Ca, Mg and Al. For P and K, only a significant correlation exists for the wet aggregate stability. As for Na and Fe, a significant positive correlation only exists for the dry aggregate stability.

Table 7: Correlation matrix for the measured aggregate stabilities and chemical properties

Chemical properties	*Wet aggregate stability **	*Dry aggregate stability **
%C	0.415*	0.544**
P	0.331*	0.215
%N	0.421*	0,585**
K	0.459*	0.091
Ca	0.063	0.249
Mg	0.173	0.124
Na	0.186	0.465**
CEC	0.430*	0.657**
Al	0.021	-0.122
Fe	0.186	0.455*

* significant relation at α=0.1 ; ** significant relation at α=0.1 with p<0.01

4.3 Multi-variate linear regression model

A multi-linear regression was performed between aggregate stability and the soil chemical properties. Initially, all soil chemical variables were used in the regression and subsequently weak independent variables were removed that expressed little relevance to the model. This multi-linear regression was done for both wet-and dry aggregate stability. For the wet aggregate stability, the following regression model was obtained:

$$AGG.STABwet = -2.9 + 0.18C + 0.0135P + 0.92\mathrm{K} + 0.42\mathrm{C} + 0.127\mathrm{Fe} \quad (22)$$

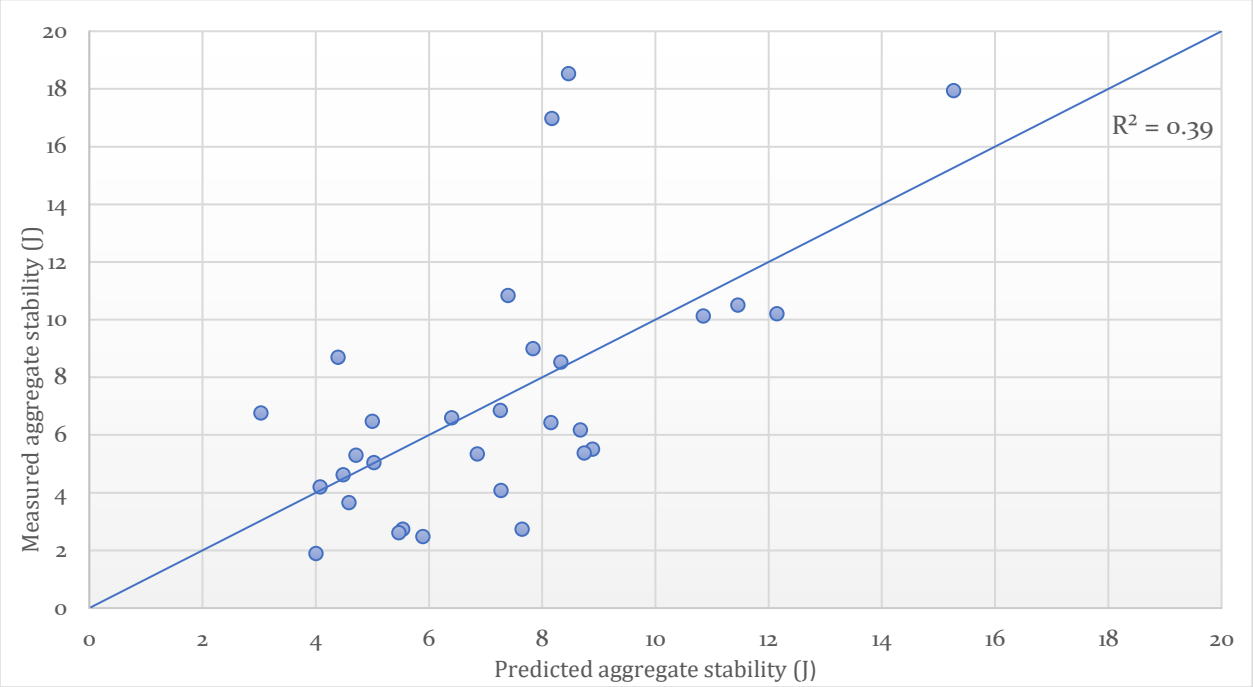

Figure 8: Multi-variate model for wet aggregate stability

The predicted wet aggregate stabilities that result from this model were plotted against the actual measurements (figure 8). The linear model proved itself significant (F=0.028), but with a weak R^2 = 0.39. When reviewing the individual coefficients, K and CEC control the predicted outcome the most. It is however a weak fit, which is mainly caused by three outliers. These three measurements had aggregate stabilities exceeding 15 J, and were removed in a new regression analysis (figure 9). With R^2=0.49, a better fit is realized for the same model parameters. It is however still a relatively weak fit.

The same procedure was applied for dry aggregate stability. The relation is defined as follows:

$$AGG.STABdry = -8.3 + 1.24C + 0.069Ca + 137Na + 0.30Fe \quad (23)$$

The predicted aggregate stabilities were again plotted against actual measurements, in order to illustrate its predictive capability (figure 10). With a R^2 of 0.70, a well fitted significant model is realized for the dry aggregate stability. Overall, the model approaches the measurements very well. The variables that had proven themselves most relevant in the correlation matrices (table 7), also came out strongest in the multi-linear regression. It is however remarkable that for Ca, no significant correlation was found for the individual regressions, but does have a significant role in this model. On the contrary, N and CEC were not incorporated into the linear model even though these variables were significant in the correlation matrix.

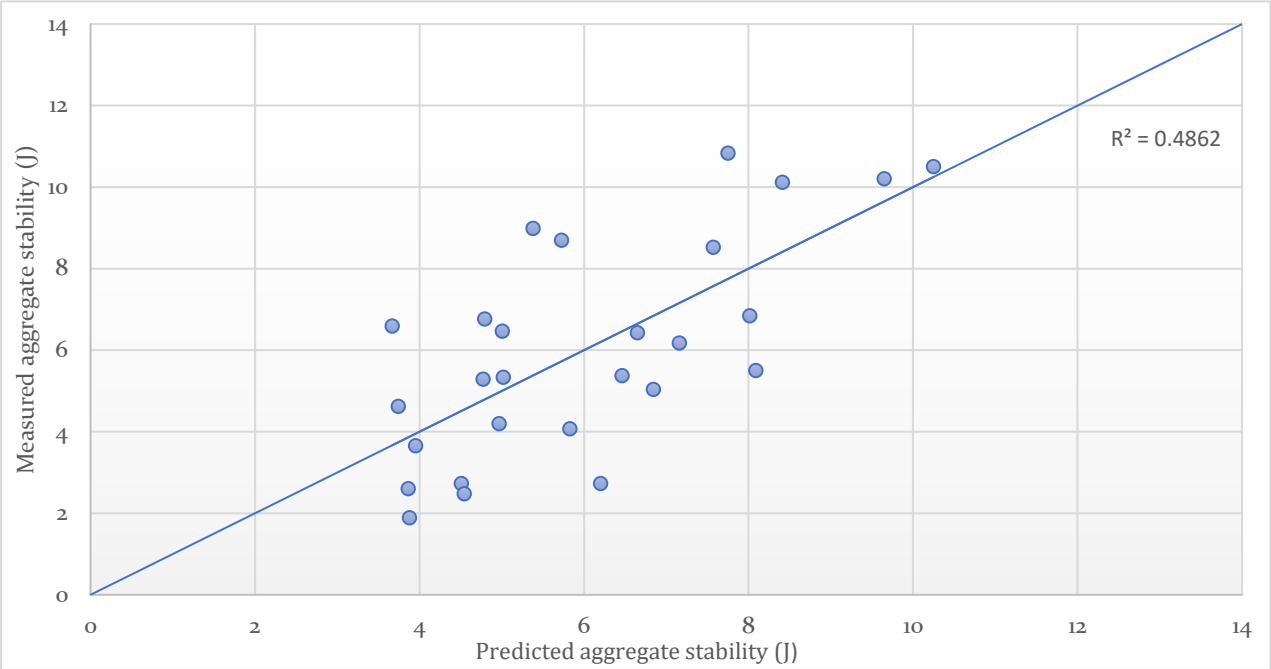

Figure 9: Multi-variate model for wet aggregate stability with outliers removed

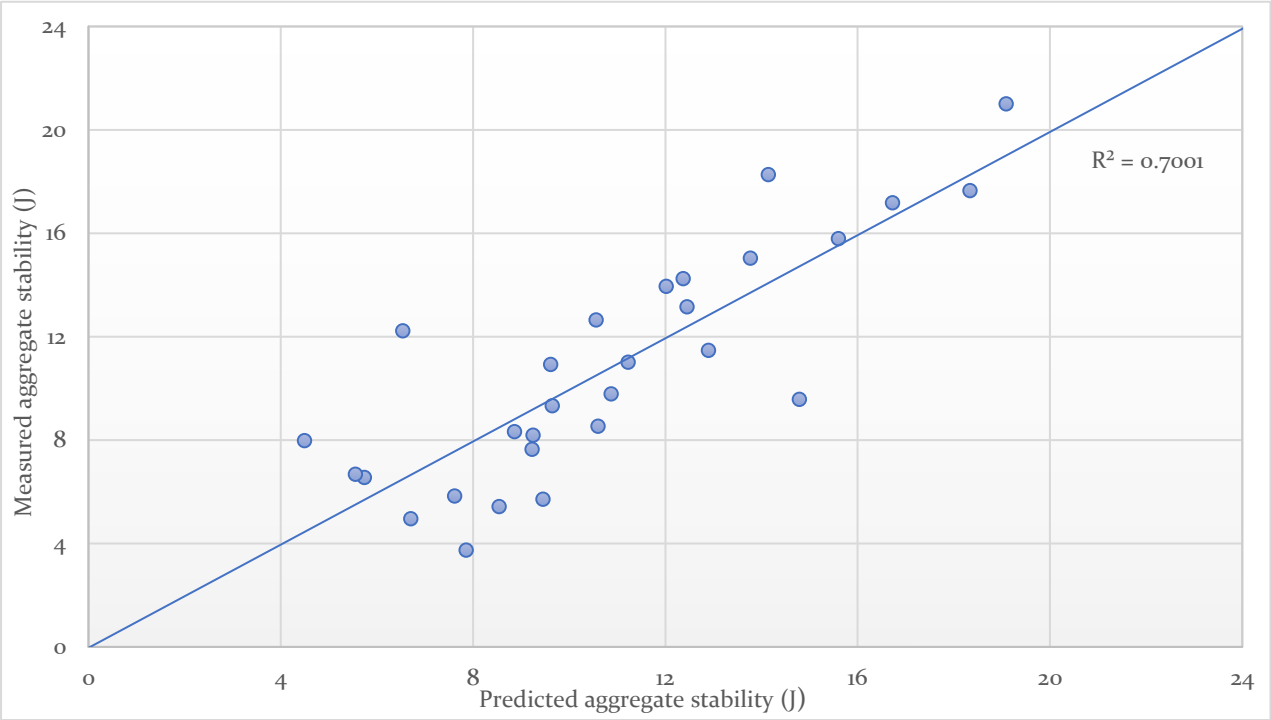

Figure 10: Multi-variate model for dry aggregate stability

Finally, a multi-variate model for dry aggregate stability was made with variables C and Fe. This resulted in a weaker fit (R^2=0.6), but C and Fe are both strong significantly correlated in this model (figure 11). The following regression coefficients apply;

$$AGG.STABdry = -6.1 + 1.47C + 0.32Fe \quad (24)$$

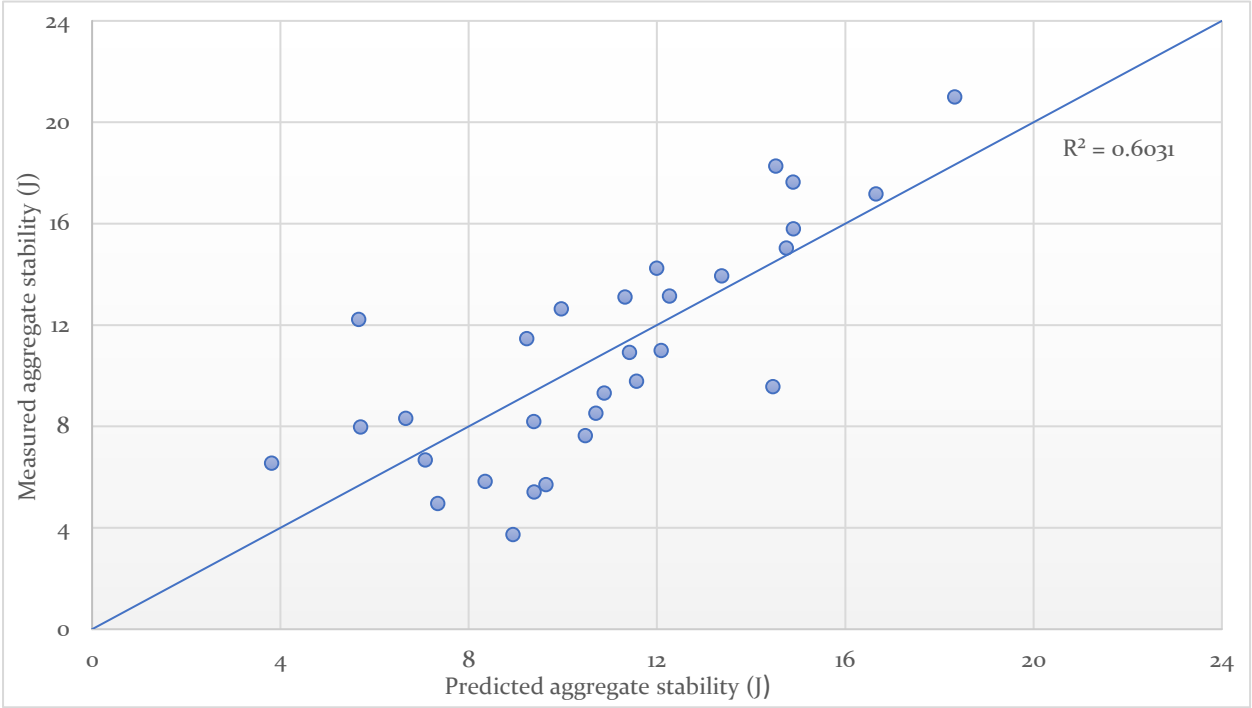

Figure 11: Multi-variate model for dry aggregate stability based on only C and Fe

Clay mineralogy

In total, 10 samples (5 erodible, 5 non-erodible) were evaluated on its clay mineralogy content using the XRD analysis (appendix C). First, a quick scan was performed for each sample. This provided a first indication of where the minerals are located in the spectrum. When evaluating the quick scan for all of the samples, two important observations were quickly made; 1) the reflection peaks (d-spacings) all show a high reciprocal resemblance 2) there are no peaks before 9 Å visible for any of the samples. This already eliminated a broad selection of potential clay minerals present in the soil. Concluding from the quick scans, full individual runs were measured starting from 9 Å.

All of the samples contained a significant amount of quartz minerals. Quartz was used here as reference to which the spectrum was corrected. When comparing the results to the automatic clay mineral database, several kaolinite clay minerals came forward which are summarized in the legend (appendix C). The main differences observed between the samples are peak intensities, but all samples have coinciding reflection patterns. The most consistent resemblance is visible in the peak around 7 A, which is clearly present within each sample. This peak is a prominent feature of the kaolinite clay group and serves as an adequate identifier for this type of mineral (Grim, 1953). Within the kaolinite clay group, several sub members were distinguished such as 'dickite' and 'nacrite'. These vary however minor in structure. Concluding, all samples contain mainly kaolinite clay, and no differences between the erodible- and non-erodible fields in clay mineralogy were observed.

4.4 rMMF model extension for aggregate stability

It was chosen to implement an increase in effective hydrological depth (EHD) ranging from 0.05-0.011 for increasing aggregate stabilities. The modelled outcomes turned out highly sensible to the EHD. According to Morgan (2005), the EHD for a bare soil with crust is 0.05, and for a bare soil without crust this is 0.09. Crusting is caused by the breakdown of aggregates, where the small particles from broken aggregates form a crust on the soil which decreases infiltration (Le Bissonnais and Arrouays, 1997). The EHD is therefore coherent to aggregate stability, which was accounted for in this model.

Modelled outcomes for erodible- to non-erodible aggregate stabilities (drop index) have been plotted against soil loss (ton/ha) and runoff (mm) in figure 12. The general trend for higher aggregate stability leading to decreased soil loss and runoff has been accurately demonstrated by the model. Here, the fastest decrease for both soil loss and runoff occurs between 20-30 drops. From here on, the decreasing trend slightly becomes more stable. In general, annual soil loss amounts range between 4-13 ton/ha.

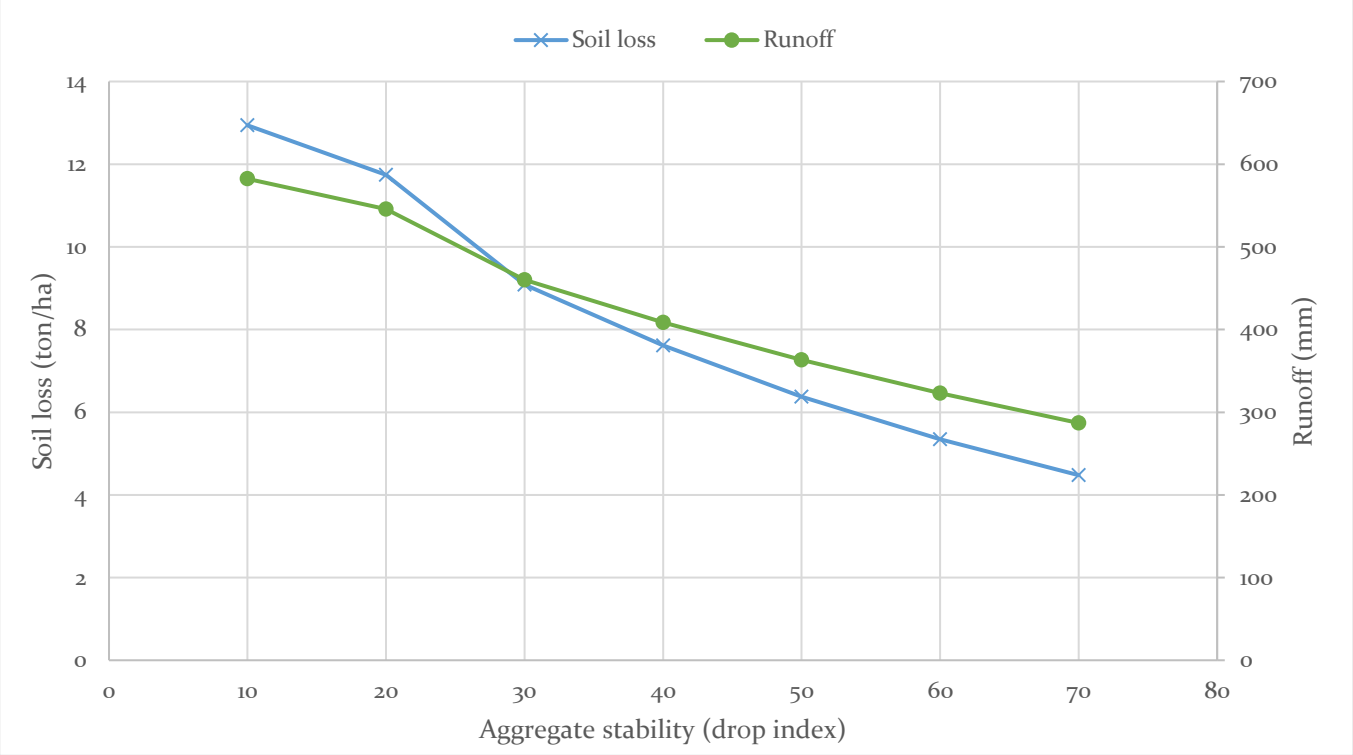

Figure 12: Soil loss and runoff in relation to aggregate stability for the rMMF model

5. Discussion

5.1 Soil physical properties

Soil texture core samples were taken for two depths at every field. The dominant texture class is clay, where some samples had higher sand- and silt contents. Statistical analysis for both clay-sand- and silt contents depicted that there were no significant differences between the erodible- and non-erodible fields. These results are not aligned with literature, where the general consensus yields a higher aggregate stability with increasing clay content and decreasing silt- and sand content. (Wischmeier and Mannering, 1969). However, Le Bissonnais and Singer (1993) did not observe a significant correlation between soil texture and aggregate stability when reviewing a wider range of soils. This observation may explain the absence of significant correlations in this study, as all of the fields are clay-dominated. Clay is generally assumed to act as a cementing factor which enhances the aggregate bonding. Since the clay content is high in all of the concerning soils, the potential negative effects of different sand- and silt fraction may not come forward since the clay fraction sufficiently strengthens the soil.

According to Imeson and Vis (1984), wet aggregates are considered highly erodible when disrupted after a maximum of 30 drops (~6.3 J). The erodible Lushoto fields have wet aggregate stability indices ranging between 10-30 drops, therefore corresponding quite well to the erodibility classification made by Imeson and Vis (1984). For the non-erodible soils, wet aggregate stability between 30-50 drops (6.3-10.5 J) can indeed be classified as low erodible. The kinetic energy from rainfall that causes disruption of the aggregate is only sufficient up to 40-50 drops; from here on, the bonds of the aggregate are considered not to be broken by individual rain drop impacts (Imeson and Vis, 1984).

The dry aggregate stability indices for the non-erodible fields range between 40-100 drops (8.4-21 J), meaning the majority of the aggregates withstood the threshold of breakdown by raindrop impact. Therefore, the non-erodible fields indeed have a low susceptibility to erosion. It must be mentioned that testing the aggregate stability according to the CND test might lead to an underestimation. Aggregates in the field naturally surround each other, being partially protected from rainfall. Since the CND method tests isolated aggregates, the realistic aggregate stability is potentially higher (Bossuyt et al., 2001).

5.2 Soil chemical properties

Soil organic matter (SOM)

The erodible fields contained significantly lower amounts of C, N and P than the non-erodible fields. The correlations that were made for soil organic carbon (C) to both the wet- and dry stabilities all came out positive and significant, being especially strong for the dry aggregate stability. The same applies for nitrogen (N), whereas only for wet aggregate stability a correlation with phosphorus (P) was found. These variables are all associated with soil organic matter (SOM), which has been an important topic of interest with regard to aggregate stability. Numerous other studies performed on the relation of SOM and aggregate stability have found similar results (Emmerson and Greenland, 1990; Chaney and Swift, 1984; Mbagwu and Piccolo, 1989).

SOM strengthens aggregate stability through its hydrophobic nature caused through the aliphatic C-H groups (humic acids). A higher content of humic acids thus causes a higher soil hydrophobicity, decreased wettability of aggregates, resulting in a slower rates of wetting and thus the degree of slaking (Sullivan, 1990). SOM also increases the cohesion of the aggregates through binding of minerals to polyvalent organic polymers (Chenu et al., 1994). As SOM

consists mainly out of C, this could be considered the most influential soil organic parameter with regard to aggregate stability.

Soil chemical variables

A strong positive correlation was found between dry aggregate stability and sodium (Na), whereas this correlation does not exist for wet aggregate stability. The significant positive correlation found for sodium and dry aggregate stability was not expected to exist prior to this study. In many studies, it had been proven that sodium induces swelling and dispersion of clay particles. Furthermore, it also leads to enhanced slaking of unstable aggregates (Crescimanno et al., 1995). This effect can partially be explained by the mono-valence of Na ions which promotes the repulsive forces within the aggregate. Furthermore, the non-erodible fields also contained significantly higher amounts of sodium than the erodible fields.

An explanation for the difference in wet- and dry aggregate stability with Na could be given by the outcomes of the research by Dexter and Chan (1991). They suggested that Na cations mostly cause clay dispersion in water, whilst enabling a strong aggregate stability in dry soils. This could potentially indicate why the wet-aggregate stabilities in the correlation matrix show different relations with sodium. However, the obtained Na values are generally very low for all six fields, which makes it therefore arguable whether a conclusive theory of Na and aggregate stability can be formed.

A strong positive correlation was found for potassium (K) and wet aggregate stability (R=0.459**). Also, a significantly lower amount of K was observed for the erodible fields. This cation is similar to Na as it is characterized by its mono-valence and therefore assumed to increase erodibility. A study conducted by Martin (1988) revealed a linear increase in erodibility with increasing K in soils. However, Levy and Torrento (1995) found opposing results where K inhibited clay dispersion and sustained aggregate stability.

Here, positive effects were attributed to the lower hydration energy of K compared to Na, which translates into a less dispersive cation. Research performed by Agboola and Corey (1973) indicated a positive correlation between K and SOM, where the SOM contributes to a better retention of K cations in the soil. This finding could also explain the positive correlation and differences for the erodible- and non-erodible fields found for K in this study. Levy and van der Watt (1990) observed a more intermediate effect of K where it stabilizes less than Ca but more than Na. Hence, the role of K in soil erodibility remains unclear as different studies on its performance delivered deviating results. It is therefore advisable to perform more research on this chemical variable since its behavior regarding aggregate stability may be unpredictable and not suitable to base firm conclusions on.

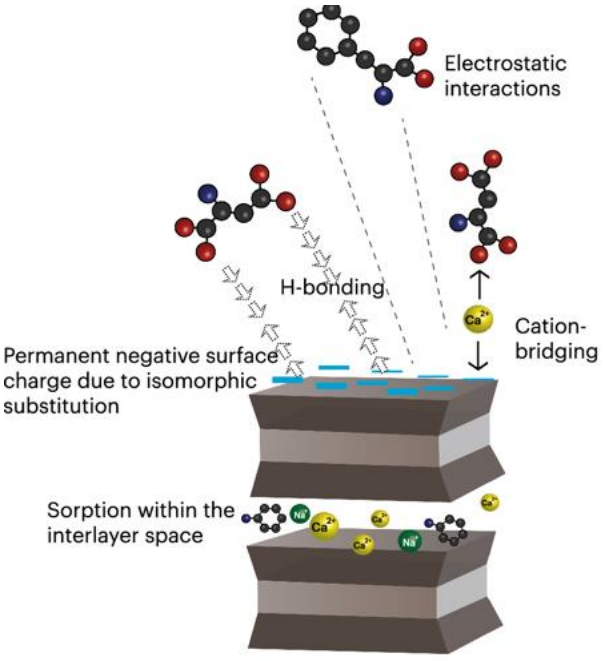

Figure 13: Clay mineral binding mechanisms (Jilling et al., 2018)

Cation exchange capacity (CEC) came forward as the strongest positive variable in relation with dry aggregate stability (r=0.657**). It also yields a positive significant relation for wet

aggregate stability (0.430*). These results are supported by findings from the study of Dimoyiannis et al., (1998), who also found that CEC was strongly correlated to better aggregate stability. A higher CEC implies a better capacity to retain the exchangeable cations in the soil (Ross and Ketterings, 1995). Figure 13 illustrates the effect of a higher CEC, which means a higher negative surface area for bonding with cations. The obtained CEC values are generally low, which could be due to the presence of mainly non-expanding minerals, such as kaolinite (Igwe, 2008). Soils generally contain greater CEC due to higher OM values and clay minerals (Ross and Ketterings, 1995). Here, the SOM might therefore indirectly contribute to a better aggregate stability.

Various studies conducted on the performance of iron and aluminum oxides indicated that their presence led to a higher stability of the aggregates (Goldberg et al., 1990; Keren and Singer 1989). Several other studies have indicated that Fe supports aggregate stability in tropical soils (Le Bissonnais, 1990; Amezketa, 1996). The positive correlation found for Fe with dry aggregate stability could confirm these stabilizing effects. There were however no significant differences in Fe content found between the erodible- and non-erodible fields.

Fe correlated well with dry aggregate stability, but no significant correlation with wet aggregate stability was obtained. A possible explanation for the contradictory results for variable Fe could be due to different analyzing methods used. The correlation matrix relates individual aggregates stabilities to individual Fe content for one sampling location. Statistically testing differences in total Fe content between the erodible- and non-erodible fields neglects the independent varying aggregate stabilities. Concluding, the observed difference in aggregate stability between the erodible-and non-erodible fields might not be influenced by total Fe content, but individual aggregate stability values to individual Fe values indicate a strong correlation.

The degree of clay dispersion of flocculation partially depends on the soil's pH (Amezteka, 1999). Results on the pH values for the six fields revealed a significant difference between the erodible- and non-erodible fields. Here, the erodible fields had a significantly higher pH. This observation is confirmed by the research performed by Chorom et al. (1994), who found that clay dispersion is stimulated with increasing pH values. However, all six study fields can be classified as acid soils based on their pH values (Baize, 1993). Despite the significant difference, it must be questioned if the differences in pH are large enough to contribute to varying aggregate stability since the soils are all classified in the same acidity range.

5.3 Clay mineralogy

It was clear that kaolinite dominated all of the samples, meaning no differences in clay mineralogy exist between the erodible- and non-erodible fields. Kaolinite is a 1:1-layer type of clay mineral which is typical for the highly weathered Usambara soils. Figure 14 illustrates the clay structure of kaolinite, where the tetra-and octahedral layer are stacked upon each other forming a 1:1 structure. When comparing kaolinite to the 2:1 clay structures in figure 14, it is apparent that kaolinite does not contain inter-surface layers where water or cations might be bound to. The absence of such inter-surface layers clarifies many of the obtained results in this study. It causes a low CEC, since the negative surface area is low as less binding opportunities are present. More importantly, it explains the dubious results on the exchangeable cation correlations.

The positive correlations for Na and K to aggregate stability might result from the absence of inter-surface layers (figure 13), as the repulsive forces due to mono-valence usually occur in these negative inter-clay layers, rather than on the negative clay edges. This theory also supports the

absence of correlations for Ca and Mg, since fewer opportunities exist for cation binding in 1:1 clay minerals.

Also common for these types of soils is a large amount of variably-charged minerals present (Denef and Six, 2005). Here, aggregate formation is partly induced through electrostatic attractions between oxides and kaolinite platelets as both positive and negative charges exist (Six et al., 2000). Hence, oxides act as a dominating binding agent through mineral-mineral bindings. This supports the significant positive correlations with Fe oxides, but also explains the moderate strength of the correlation with C.

For kaolinite clay dominated soils, a lower correlation between aggregate stability and C exists. This was also observed by Six et al., (2002), who reported that for soils in tropical regions dominated by 1:1 clay minerals and oxides, a higher aggregate stability exists but with lower correlation for C and aggregate stability. Organic polymers are polyvalent binding agents, which function much better at a higher CEC with greater negative surface area. Hence, a moderate correlation for C was found in this study, as the oxides are the favorable binding agent for the 1:1 clay minerals, where a lower CEC thus negative surface area exists.

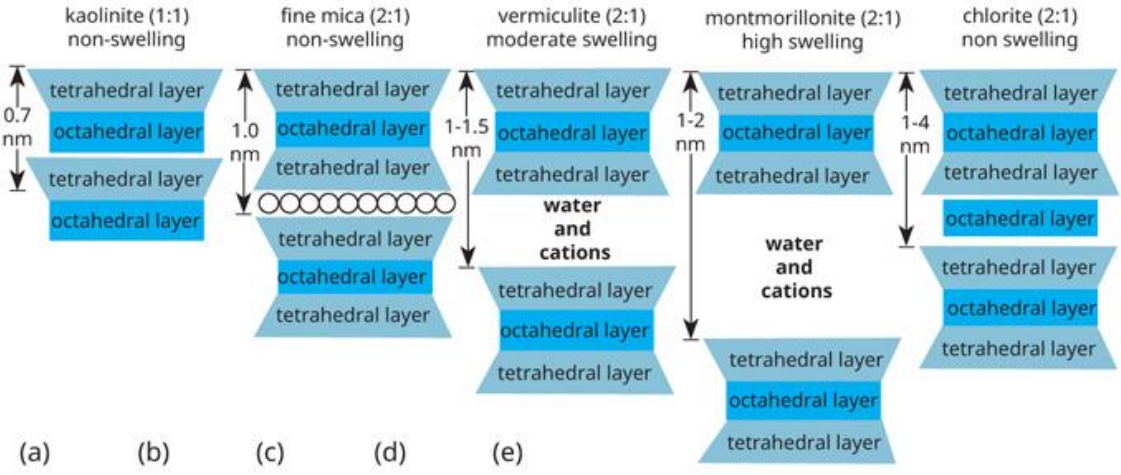

Figure 14: Clay mineral structures (Brady et al., 2002)

5.4 Multi-variate models

The multi-variate models that were made for wet-and dry aggregate stability differ highly in their goodness of fit. The wet aggregate stability model predicts the stabilities in a lesser amount, with a R^2=0.39. Hence, a correction on the dataset was performed in order to achieve a better fit. The outlying values were removed from the analysis. A slightly better fit was realized for the new regression model (R^2 =0.48) The individual p-values however revealed that almost no significant variables exist in this model. It is therefore difficult to predict the wet aggregate stability based on the acquired model, as many data points seem highly variable and inconsistent.

As for the dry aggregate stability, two well-fitted multi-variate model were derived. It is not surprising that such better performing models could be realized when reviewing the correlation matrix. The individual correlations are much stronger and higher in significance between the variables and dry aggregate stability. This allows for an easier predictive model. The dry AGG.STAB multi-variate model with variables Fe and C showed the highest significance for the individual variables. This is consistent with the individual correlations and confirms both the SOM and oxide aggregate bindings.

However, variables CEC and N are absent in both models, despite having individual positive correlations to dry aggregate stability. This could be explained by the interactive behavior of the variables. The multi-linear regressions suggest that the strength of variables CEC and N decrease when combined with the other variables in relation to aggregate stability. The individual variance for both variables may not affect the individual regressions, but could be much more substantial in comparison to the other variables. Hence, the relevance of these variables could be significantly reduced in a multi-linear regression. Opposing to this, variable Ca is only significantly correlated to dry aggregate stability in the multi-variate model. Here, the exact opposite applies, where Ca relies on the other variables in order to significantly contribute to a better aggregate stability.

It is interesting to debate on the inconsistency of the wet aggregate stability. Research performed by Reichert (2009) indicated that for kaolinite- and oxide dominated soils the breakdown of aggregates is mainly induced by fast wetting. These findings could explain the inconsistency for the wet aggregate breakdown, since the dry aggregates are more susceptible for the primary breakdown mechanism in these kaolinitic soils. Therefore, it may exert a higher correlation to favorable soil composition as this may better inhibit the breakdown mechanism. The soil chemical composition of the wet aggregates could be of less importance since a different type of mechanism is acting upon it.

Most importantly, the fast wetting of an aggregate (slaking) is a more realistic aggregate breakdown mechanism as it closest resembles field conditions (Bossuyt et al., 2001). Rainfall events in the Lushoto area are usually short and intense. This implies a rapid wetting of the aggregates, but due to the short duration there is a possibility of air drying. Hence, analyzing the dry aggregate stability represents the most realistic behavior of the aggregates in the field.

5.5 rMMF model with the aggregate stability function

The updated rMMF model with aggregate stability component functions appropriately when compared to the previous model. In general, the soil erosion values have decreased slightly, but are still in range with the modelled outcomes from the rMMF model without the aggregate stability function (appendix D). The fastest decrease in runoff and soil loss corresponds to the transition between 20-30 drops, which corresponds to the transition of erodible- to non-erodible aggregate stability index. The erosion values range between 4 -10 ton/ha, which is lower than erosion rates reported in literature regarding the Usambara Mountains (Buch, 1983). This may be due to the β-value used in the model, which influences the outcomes in a substantial way. When accurate sediment transport values are available, the β-value could be derived from calibration.

It is however important to understand the implications of the varying EHD in relation to aggregate stability on the modelled outcomes. Research performed by Gorter (2013) has shown that the non-erodible fields experience higher infiltration compared to the erodible fields. This effect is accounted for by increasing the EHD values for higher aggregate stability. Better infiltration leads to lower surface runoff and transport capacity. This would implicate a greater relevance of variable hydrological conditions in the model, rather than the actual splash detachment.

The implementation of the aggregate stability component used earlier by de Roo (1996) thus appears to function well within the rMMF model. It remains however arguable if this relation is suitable for annually based models, since it has undergone several adaptions. The function itself is however plausible, as it is still based upon total rainfall and kinetic energy when estimating

the splash detachment. By changing the rainfall detachment section in the rMMF with the new function, the general detachment processes are kept in order but an important soil parameter is now incorporated in the calculations. The aggregate stability function could be even further optimized if the clay type- and amount are incorporated, as suggested by Morgan and Duzant (2008).

6. Conclusions

The erodible fields contained a significantly lower amount of SOM (C, N and P) than the non-erodible fields. No significant differences were found for Ca, Mg, Al and Fe content between the two types of fields. Positive correlations were obtained for %C, %N, and CEC for both wet- and dry aggregate stability. For wet aggregate stability, both P and K were also found significantly correlated. For dry aggregate stability, this included Na and Fe. No conclusive theory could be formed for the exchangeable cations in relation to aggregate stability. Kaolinite clay dominates all six fields, which contains small negative surface area (CEC) and absence of inter-surface layers. Binding of polyvalent cations is therefore also less pronounced for these soils. Furthermore, the absence of inter-surface layers explains why no negative effects of monovalent ions (Na and K) on aggregate stability were noticed. Concluding, both Fe and SOM have a significant, positive influence on aggregate stability in the Usambara region. For the erodible- and non-erodible fields, the SOM content is the dominant factor in controlling the aggregate stabilities.

Multi-linear regressions led to the formations of predictive models for both wet-and dry aggregate stability. Here, the dry aggregate stability model performed much better than the wet aggregate stability model. This is assumed to be caused by a stronger response of dry aggregates to favorable soil composition. Kaolinite soils primary experience aggregate breakdown by fast wetting (slaking), which mostly concerns dry aggregates. Hence, dry aggregates may correspond more consistently to better soil conditions inducing stronger correlations.

Finally, an aggregate function was implemented in the rMMF erosion model. The modelled outcomes became slightly lower compared to the original model. Increasing aggregate stabilities were assumed to increase EHD values, which resulted in lower modelled erosion outcomes. Variable hydrological conditions affect modelled outcomes the most. Since the newly implemented function still resembles rainfall detachment processes, a plausible adaption was made.

References

Agboola, a. & Corey, B. (1973): *The relationship between soil Ph, organic matter, available phosphorus, exchangeable potassium, calcium, magnesium, and nine elements in the maize tissue.* Soil Science. 115. 10.1097/00010694-197305000-00006

Amezketa, E. (1999). *Soil aggregate stability: a review*. Journal of sustainable agriculture, 14(2-3), 83-151.

Baize, D. (1993). *Soil science analyses. A guide to current use*. John Wiley & Sons Ltd. West Sussex.

Bergaya, F., Lagaly, G., (2006). *General introduction: clays, clay minerals, and clay science*. In: Bergaya, F., Theng, B.K.G., Lagaly, G. (Eds.), Developments in Clay Science, first ed., vol. 1. Elsevier, Amsterdam, pp. 1e18 (Chapter 1).

Berry, L., Turner, B. (1990). *The Earth as transformed by human action*. Science: CUP Archive, 713 pages

Bissonnais, Y. Le, Arrouays, D. (1997). *Aggregate stability and assessment of soil crustability and erodibility: II. Apllication to humic loamy soils with various organic carbon contents*. European Journal of Soils Science 48: 39-48.

Le Bissonnais, Y. (1988). *Analyse des mecanismes de desagregation et de la mobilisation des particles de terre sous l'action des pluies*. These de Doctorat, Universite d'Orleans.

Le Bissonnais, Y. (1996). *Aggregate stability and assessment of soil crustability and erodibility I. Theory and methodology.* European Journal of soil science 47.4 425-437.

Bossuyt, H., Denef, K., Six, J., Frey, S. D., Merckx, R., & Paustian, K. (2001). *Influence of microbial populations and residue quality on aggregate stability*. Applied Soil Ecology, *16*(3), 195-208.

Boxtel, van J. H. (1997). *Numerical model for the fall speed of rain drops in a rain fall simulator*. In Workshop on wind and water erosion (pp. 77-85).

Bouyoucos, G. J. (1962). *Hydrometer method improved for making particle size analyses of soils* 1. Agronomy journal, 54(5), 464-465.

Brunauer S., Emmett P. H. and Teller E. (1938). *Adsorption of gases in multi molecular layers*. J. Am. them. Sot. 60, 309-319.

Brady, NC and Weil, RR. (2002). *The Nature and Properties of Soils*. 13th ed. Prentice Hall: New Jersey.

Buch, M.W., (1983). *Semiquantitative Beschreibung von Boodenerosion an Hangen unterschiedlicher Landnutzung, Neigung und Lange in funf Dorfgebieten der Westlichen Usambara-Mts, Tanzania*. Studie-SECAP (Lushoto), Eschborn, Germany.

Cerda, A. (1998). *Soil aggregate stability under different Mediterranean vegetation types*. 73–86.

Chaney, K., & Swift, R. S. (1984*). The influence of organic matter on aggregate stability in some British soils.* Journal of Soil science, 35(2), 223-230.

Chapman, H.D. (1965). *Cation exchange capacity.* In C.A. Black et al., Eds., Methods of Soil Analysis. Agronomy 9, American Society of Agronomy, Madison, WI, pp. 891–901

Chappell, N. A., Ternan, J. L., & Bidin, K. (1999). *Correlation of physicochemical properties and sub-erosional landforms with aggregate stability variations in a tropical Ultisol disturbed by forestry operations*. Soil and Tillage Research, 50(1), 55-71.

Chenu, C., Y. Le Bissonnais, and D. Arrouays (2000*). Organic matter influence on clay wettability and soil aggregate stability*. Soil Science Society of America Journal 64.4): 1479-1486.

Chenu, C. & Cosentino, D. (2011). *Microbial Regulation of Soil Structure Dynamics.* 10.1079/9781845935320.0037.

Chenu, C. and J. Guerif. (1991). *Mechanical strength of clay minerals as influenced by an adsorbed polysaccharide*. Soil Sci. Soc. Am J. 55:1076–1080

Chenu, C., J. Gue´rif, and A.M. Jaunet. (1994). *Polymer bridging of clay and soil structure stabilization by polysacchrides*. p. 403–410. In XVth World Congress of Soil Science, 3a. ISSS, Accapulco, Mexico

Chisci G, Bazzoffi P, Mbagwu JSC. (1989). *Comparison of aggregate stability indices for soil classification and assessment of soil management practices*. Soil Technology 2: 113–133.

Christensen, N. L., Wilbur, R. B., & McLean, J. S. (1988). *Soil-vegetation correlations in the pocosins of Croatan National Forest, North Carolina* (No. FWS-88 (28).

Chorom, M., & Rengasamy, P. (1995). *Dispersion and zeta potential of pure clays as related to net particle charge under varying pH, electrolyte concentration and cation type*. European Journal of Soil Science, 46(4), 657-665.

Conte, CA. (1999). *The forest becomes desert: forest use and environmental change in Tanzania's West Usambara Mountains*. Land Degradation & Development 10: 291–309

Dalal, R. and R.J. Mayer (1986). *Longterm trends in fertility of soils under continuous cultivation and cereal cropping in Queensland. II. Total organic carbon and its rate of loss from soil profile*. Australian Journal of Soil Research 24, 301-309

Denef, K., and J. Six (2005). *Clay mineralogy determines the importance of biological versus abiotic processes for macroaggregate formation and stabilization*. European Journal of Soil Science 56.4 469-479.

Dimoyiannis, D. G., Tsadilas, C. D., & Valmis, S. (1998). *Factors affecting aggregate instability of Greek agricultural soils*. Communications in Soil Science and plant analysis, 29(9-10), 1239-1251.

Dixon, J.B. & Weed, S.B. (1989). *Minerals in Soil Environments*. Soil Science Society of 518 America Inc., Madison.

Dutrow, Barb, (1997). *Better Living Through Minerals X-ray Diffraction of Household Products*, in: Brady, J., Mogk, D., and Perkins D. (eds.) Teaching Mineralogy, Mineralogical Society of America, p. 349-359

Emerson, W.W. & Greenland, D.J. (1990). *Soil Aggregates-Formation and stability*. In: Soil colloids and their associations in aggregates (eds M. De Boodt, M. Hayes & A. Herbillon), pp. 485-51 1. Plenum Press, New York

Ezaza, W. (1988*). Geo-ecological factors influencing over-exploitation and land degradation in the Usambara Mountains of northeastern Tanzania*. Mountain research and development 8: 157-163.

Farres, P.J. (1987). *The dynamics of rainsplash erosion and the role of soil aggregate stability.*

FMANR (Federal Ministry of Agriculture and Natural Resources) 1990. *Literature review on soil fertility investigations in Nigeria*. Bobma Publishers, Ibadan Nigeria. Catena, 14, 119-130.

German, L., Mazengia, W., Taye, H., Tsegaye, M., Ayele, S., Charamila, S., & Wickama, J. (2010). *Minimizing the livelihood trade-offs of natural resource management in the Eastern African Highlands*: policy implications of a project in "creative governance". Human Ecology, 38(1), 31-47.

Goldberg, S. & H.S. Forster (1990). *Flocculation of reference clays and arid-zone soil clays*. Soil Sci. Soc. Am. J. 54:714-718

Google Earth imaging (2019)

Gorter, L (2013). *Soil physical properties in relation to soil degradation rates in the Usambara Mountains, northeast Tanzania.* MSc thesis, Utrecht University

Harpum, J. R. (1963). *Petrographic classification of granitic rocks by partial chemical analysis*. Tanganyika Geological Survey 10 80-88.

Hartemink, A. E. (1997). *Soil fertility decline in some major soil groupings under permanent cropping in Tanga region, Tanzania*. Geoderma, 75(3-4), 215-229.

Haynes, R. J., & Swift, R. S. (1990). *Stability of soil aggregates in relation to organic constituents and soil water content*. Journal of soil science, 41(1), 73-83.

Herweg, Karl (1996). *Field manual for assessment of current erosion damage*. University of Berne

Jankauskas, B., Jankauskienė, G., Fullen, M.A. (2008). *Soil erosion and changes in the physical properties of Lithuanian Eutric Albeluvisoils under different land use systems*. Acta Agriculturae Scandinavica, Section B - Plant Soil Science 58: 1, 66-76.

Jilling, A., Keiluweit, M., Contosta, A. R., Frey, S., Schimel, J., Schnecker, J., ... & Grandy, A. S. (2018). M*inerals in the rhizosphere: overlooked mediators of soil nitrogen availability to plants and microbes*. Biogeochemistry, 139(2), 103-122.

Igwe, C. A., & Udegbunam, O. N. (2008). *Soil properties influencing water-dispersible clay and silt in an Ultisol in southern Nigeria*. International Agrophysics, 22(4), 319-325.

Kaswamila AL, Tenge AJ. (1998*). The Neglect of Traditional Agroforestry and its Effects on Soil Erosion and Crop Yields. The Case of West Usambara Highlands*. Research on Poverty Alleviation (REPOA). DSM, Tanzania

Kemper, W. D., and R. C. Rosenau (1986). *Aggregate stability and size distribution*. 425-442.

Keren, R. & M.J. Singer (1989). *Effect of low electrolyte concentration on hydraulic conductivity of clay-sand-hydroxy polymers systems*. Soil Sci. Soc. Am. J. 53: 349-355.

Lal, R., (1985). *Soil erosion and sediment transport research in tropical Africa*. Hydrological Sciences Journal 30, 117}134

Lavee, P. Sarah & A.C. Imeson (1996). *Aggregate Stability Dynamics as Affected by Soil Temperature and Moisture Regimes*, Geografiska Annaler: Series A, Physical Geography, 78:1, 73-82

Levy, G. J., & Torrento, J. R. (1995). *Clay dispersion and macroaggregate stability as affected by exchangeable potassium and sodium*. Soil science, 160(5), 352-358.

Levy, G. J., & Van Der Watt, H. V. H. (1990). *Effect of exchangeable potassium on the hydraulic conductivity and infiltration rate of some South African soils*. Soil Science, 149(2), 69-77.

Lundgren, L., Lundgren, B. (1979). *Rainfall, interception and evaporation in the Mazumbai Forest Reserve, West Usambare Mountains, Tanzania, and their importance in the assessment of land potential*. Geografiska Annaler 61A (3-4): 157-178

Lundgren, L. (1980). *Comparison of surface runoff and soil loss from runoff plots in forest and small-scale agriculture in the Usambara Mts., Tanzania*. Geografiska Annaler 62.3-4 113-148.

Mahoo, H., Mbungu, W., Yonah, I., Radeny, M. A., Kimeli, P., & Kinyangi, J. (2015). I*ntegrating indigenous knowledge with scientific seasonal forecasts for climate risk management in Lushoto district in Tanzania.*

Mann, L.K., (1986). *Changes in soil carbon storage after cultivation*. Soil Science 142, 279–288

Makoi, J. H. J. R., & Ndakidem, P. A. (2008). *Selected chemical properties of soil in the traditional irrigation schemes of the Mbulu district, Tanzania*. African Journal of Agricultural Research, 3(5), 348-356.

Martin, W. (1988). *Die Erodierbarkeit von Boden unter simulierten und naturlichen Regen und ihre Abhangkkeit von Bodeneigenschaften*. PhD Thesis, Techn. Univ. Munich

Mbagwu, J. S. C., & Piccolo, A. (1989). *Changes in soil aggregate stability induced by amendment with humic substances*. Soil Technology, 2(1), 49-57.

McKnight, T.L., Hess, D. (2008). *Physical Geography: A Landscape Appreciation*. Pearson Prentice Hall.

Meliyo, J., J. W. Kabushemera, and A. J. Tenge (2001). *Characterization and mapping soils of Kwalei subcatchment, Lushoto District*. Mlingano Agricultural Research Institute, Tanga, Tanzania

Morgan, R.P.C., Morgan, D.D.V., Finney, H.J. (1982*). Stability if agricultural ecosystems: documentation of a simple model for soil erosion assessment*

Morgan, R.P.C. (2001). *A simple approach to soil loss prediction: a revised Morgan-Morgan-Finney model.* Catena 44: 305-322

Morgan, R.P.C. (2005). *Soil Erosion and Conservation*. Blackwell Publishing Ltd.

Morgan, R. P. C., & Duzant, J. H. (2008). *Modified MMF (Morgan–Morgan–Finney) model for evaluating effects of crops and vegetation cover on soil erosion*. Earth Surface Processes and Landforms: The Journal of the British Geomorphological Research Group, 33(1), 90-106.

Moore, D.M., Reynolds, R.C., (1997). *X-ray Diffraction and the Identification and Analysis of Clay Minerals, second ed. Oxford University Press, Oxford.*

Mwango, S. B., Msanya, B. M., Mtakwa, P. W., Kimaro, D. N., Deckers, J., & Poesen, J. (2016). *Effectiveness of mulching under miraba in controlling soil erosion, fertility restoration and crop yield in the Usambara Mountains, Tanzania*. Land Degradation & Development, 27(4), 1266-1275.

Ndakidemi, P. A., & Semoka, J. M. R. (2006). *Soil fertility survey in western Usambara Mountains, northern Tanzania*. Pedosphere, 16(2), 237-244.

Panayiotopoulos, K. P., Barbayiannis, N., & Papatolios, K. (2004). *Influence of electrolyte concentration, sodium adsorption ratio, and mechanical disturbance on dispersed clay particle size and critical flocculation concentration in Alfisols*. Communications in soil science and plant analysis, 35(9-10), 1415-1434.

Pfeiffer, R., (1990). *Sustainable Agriculture in Practice—the Production Potential and the Environmental Effects of Macro-contourlines in the West Usambara Mountains of Tanzania. University of Hohenheim, Stuttgart, Germany* (195 pp.).

Poesen J. (1985). *An improved splash transport model.* Zeitschrift für Geomorfologie 29: 193–211.

Prosser, I.P. and P. Rustomji. (2000). *Sediment transport capacity relations for overland flow.* Progress in Physical Geography 24: 179-193.

Reichert, J. M., Norton, L. D., Favaretto, N., Huang, C. H., & Blume, E. (2009). *Settling velocity, aggregate stability, and interrill erodibility of soils varying in clay mineralogy*. Soil Science Society of America Journal, 73(4), 1369-1377.

Renard, K.G., Foster, G.A., Weesies, D.A., McCool, D.K., Yoder, D.C., (1997). *Predicting Soil Erosion by Water: A Guide to Conservation Planning with the Revised Universal Soil Loss Equation (RUSLE).* Agriculture Handbook No. 703, USDA, Washington DC

Romkens, M.J.M., Roth, C.B. & Nelson, D.W. (1977*). Erodibility of selected clay subsoils in relation to physical and chemical properties*. Soil Science Society of America Journal, 41,954-960.

Ross, D. S., & Ketterings, Q. (1995). *Recommended methods for determining soil cation exchange capacity*. Recommended soil testing procedures for the northeastern United States, 2, 62-70.

De Roo, A. P. J., Wesseling, C. G., & Ritsema, C. J. (1996). *LISEM: a single-event physically based hydrological and soil erosion model for drainage basins. I: theory, input and output. Hydrological processes*, 10(8), 1107-1117.

Scheinmann, D., (1986). *Caring for land of Usambara. A guide to preserving the environment through agriculture, agroforestry and zero grazing*. SECAP, Lushoto, Tanzania

Schulten, H. R., Leinweber, P., & Sorge, C. (1993). *Composition of organic matter in particle-size fractions of an agricultural soil. Journal of soil science,* 44(4), 677-691.

Siband, P., (1974). *Evolution des caractères et la fertilité d'un sol rouge de Casamance.* Agronomie Tropicale 29, 1228–1248

Six, J., Conant, R. T., Paul, E. A., & Paustian, K. (2002). *Stabilization mechanisms of soil organic matter : Implications for C-saturation of soils*, 155–176.

Sterk, G., (2019). *A hillslope version of the revised Morgan, Morgan and Finney water erosion model.*

Sullivan, L.A. (1990). *Soil organic matter, air encapsulation and water stable aggregation*. J. Soil Sci. 41:529–534.

Tanzania National Consensus (2014). *Consensus estimates on key population size and HIV prevalence in Tanzania.*

Tate, K. R., & Theng, B. K. G. (1980). *Organic matter and its interactions with inorganic soil constituents.* Soils with variable charge, 225-249.

Tenge, A. J., De Graaff, J., & Hella, J. P. (2004). *Social and economic factors affecting the adoption of soil and water conservation in West Usambara highlands, Tanzania.* Land Degradation & Development, 15(2), 99-114.

Tisdall, J.M., and J.M. Oades. (1982). *Organic matter and water-stable aggregates*. J. Soil Sci. 33:141–163

Walkley, A., & Black, I. A. (1934). *An examination of the Degtjareff method for determining soil organic matter, and a proposed modification of the chromic acid titration method*. Soil science, 37(1), 29-38.

Walker, S.M., Desanker, P.V., (2004). *The impact of land use on soil carbon in Miombo Woodlands of Malawi.* Forest Ecology and Management 203, 345–360

Wickama, J, B. Okoba, and Sterk. G., (2014). *Effectiveness of sustainable land management measures in West Usambara highlands, Tanzania*. Catena 118): 91-102.

Wickama, J., Masselink, R., & Sterk, G. (2015). *The effectiveness of soil conservation measures at a landscape scale in the West Usambara highlands, Tanzania*. Geoderma, 241, 168-179.

Wickama, J., & Mowo, J. (2001). *Using local resources to improve soil fertility in Tanzania*.

Wischmeier, W. H., & Mannering, J. V. (1969). *Relation of soil properties to its erodibility 1*. Soil Science Society of America Journal, 33(1), 131-137.

Wischmeier, W.H., Smith, D.D. (1978) *Predicting rainfall erosion losses.* USDA Agricultural Research Service Handbook, 537

Woytek, R., Bahring, A., Dersch, D., Habermehl, J., Kauf- man, P. and Weitz, M., (1987). *Soil erosion control and agroforestry in the West Usambara Mountains.* Technical University of Berlin, Berlin, pp. 1-75

Zhou, X., Liu, D., Bu, H., Deng, L., Liu, H., Yuan, P., ... & Song, H. (2018). *XRD-based quantitative analysis of clay minerals using reference intensity ratios, mineral intensity factors*, Rietveld, and full pattern summation methods: A critical review. Solid Earth Sciences.

Zonn, S.V. (1986). *Tropical and subtropical soils science*. Mir Publishers Moscow, pp 422.

Appendices

Appendix A: Statistical analyses

Soil texture

F-Test Two-Sample for Variances

clay 0-15	*Variable 1*	*Variable 2*
Mean	53.16666667	51.33333
Variance	80.58333333	17.33333
Observations	3	3
df	2	2
F	4.649038462	
P(F<=f) one-tail	0.177021277	
F Critical one-tail	9	

F-Test Two-Sample for Variances

clay 15-30	*Variable 1*	*Variable 2*
Mean	54.83333333	51.33333
Variance	25.58333333	9.333333
Observations	3	3
df	2	2
F	2.741071429	
P(F<=f) one-tail	0.267303103	
F Critical one-tail	9	

t-Test: Two-Sample Assuming Equal Variances

clay 0-15	*Variable 1*	*Variable 2*
Mean	53.16667	51.33333
Variance	80.58333	17.33333
Observations	3	3
Pooled Variance	48.95833	
Hypothesized Mean Difference	0	
df	4	
t Stat	0.320903	
P(T<=t) one-tail	0.382175	
t Critical one-tail	1.533206	
P(T<=t) two-tail	0.76435	
t Critical two-tail	2.131847	

t-Test: Two-Sample Assuming Equal Variances

clay 15-30	*Variable 1*	*Variable 2*
Mean	54.83333	51.33333
Variance	25.58333	9.333333
Observations	3	3
Pooled Variance	17.45833	
Hypothesized Mean Difference	0	
df	4	
t Stat	1.025917	
P(T<=t) one-tail	0.181459	
t Critical one-tail	1.533206	
P(T<=t) two-tail	0.362918	
t Critical two-tail	2.131847	

F-Test Two-Sample for Variances

Sand	*Variable 1*	*Variable 2*
Mean	31.66667	36
Variance	90.33333	12
Observations	3	3
df	2	2
F	7.527778	
P(F<=f) one-tail	0.117264	
F Critical one-tail	9	

F-Test Two-Sample for Variances

Silt	*Variable 1*	*Variable 2*
Mean	10.66667	8.666667
Variance	10.58333	1.333333
Observations	3	3
df	2	2
F	7.9375	
P(F<=f) one-tail	0.111888	
F Critical one-tail	9	

t-Test: Two-Sample Assuming Equal Variances

Sand	*Variable 1*	*Variable 2*
Mean	31.66667	36
Variance	90.33333	12
Observations	3	3
Pooled Variance	51.16667	
Hypothesized Mean Difference	0	
df	4	
t Stat	-0.74195	
P(T<=t) one-tail	0.24966	
t Critical one-tail	1.533206	
P(T<=t) two-tail	0.499319	
t Critical two-tail	2.131847	

t-Test: Two-Sample Assuming Equal Variances

Silt	*Variable 1*	*Variable 2*
Mean	10.66667	8.666667
Variance	10.58333	1.333333
Observations	3	3
Pooled Variance	5.958333	
Hypothesized Mean Difference	0	
df	4	
t Stat	1.00349	
P(T<=t) one-tail	0.186203	
t Critical one-tail	1.533206	
P(T<=t) two-tail	0.372405	
t Critical two-tail	2.131847	

F-Test Two-Sample for Variances

Clay total 0-15	*Variable 1*	*Variable 2*
Mean	52.25	53.08333
Variance	40.175	17.64167
Observations	6	6
df	5	5
F	2.277279	

P(F<=f) one-tail	0.193722
F Critical one-tail	3.452982

t-Test: Two-Sample Assuming Equal Variances

Clay total 15-30	*Variable 1*	*Variable 2*
Mean	52.25	53.08333
Variance	40.175	17.64167
Observations	6	6
Pooled Variance	28.90833	
Hypothesized Mean Difference	0	
df	10	
t Stat	-0.26845	
P(T<=t) one-tail	0.396904	
t Critical one-tail	1.372184	
P(T<=t) two-tail	0.793808	
t Critical two-tail	1.812461	

Bulk density

F-Test Two-Sample for Variances

Bulk density	*Erodible*	*Non Erodible*
Mean	1.177333333	1.263666667
Variance	0.011626333	0.017182333
Observations	3	3
df	2	2
F	0.676644616	
P(F<=f) one-tail	0.40357068	
F Critical one-tail	5	
	0.11111111	

t-Test: Two-Sample Assuming Equal Variances

Bulk density	*Erodible*	*Non Erodible*
Mean	1.177333333	1.263666667
Variance	0.011626333	0.017182333
Observations	3	3
Pooled Variance	0.014404333	
Hypothesized Mean Difference	0	
df	4	
t Stat	-0.881003345	

P(T<=t) one-tail	0.214035308
t Critical one-tail	1.533206274
P(T<=t) two-tail	0.428070615
t Critical two-tail	2.131846786

STATISTICS **Dry aggregate stability**

F-Test Two-Sample for Variances

	Variable 1	*Variable 2*
Mean	7.6468	14.0756
Variance	6.3749616	12.0410304
Observations	15	15
df	14	14
F	0.529436551	
P(F<=f) one-tail	0.123177626	
F Critical one-tail	0.494453739	

Wet aggregate stability

F-Test Two-Sample for Variances

	Variable 1	*Variable 2*
Mean	4.298	10.108
Variance	2.581404	19.202316
Observations	15	15
df	14	14
F	0.134431909	
P(F<=f) one-tail	0.000292926	
F Critical one-tail	0.494453739	

t-Test: Two-Sample Assuming Equal Variances

DRY	*Variable 1*	*Variable 2*
Mean	7.6468	14.0756
Variance	6.374962	12.04103
Observations	15	15
Pooled Variance	9.207996	
Hypothesized Mean Difference	0	
df	28	
t Stat	-5.802	
P(T<=t) one-tail	1.56E-06	

t Critical one-tail	1.312527
P(T<=t) two-tail	3.12E-06
t Critical two-tail	1.701131

t-Test: Two-Sample Assuming Unequal Variances

WET	*Variable 1*	*Variable 2*
Mean	4.298	10.108
Variance	2.581404	19.20232
Observations	15	15
Hypothesized Mean Difference	0	
df	18	
t Stat	-4.82121	
P(T<=t) one-tail	6.85E-05	
t Critical one-tail	1.330391	
P(T<=t) two-tail	0.000137	
t Critical two-tail	1.734064	

t-Test: Two-Sample Assuming Unequal Variances

P	*Erodible*	*Non erodible*
Mean	10.9178	32.52006659
Variance	88.077724	3721.218274
Observations	15	15
Hypothesized Mean Difference	0	
df	15	
t Stat	-1.355572	
P(T<=t) one-tail	0.0976478	
t Critical one-tail	1.3406056	
P(T<=t) two-tail	0.1952957	
t Critical two-tail	1.7530504	

t-Test: Two-Sample Assuming Unequal Variances

K	*Erodible*	*Non-erodible*
Mean	0.522381	2.032396
Variance	1.552472	4.524702
Observations	15	15
Hypothesized Mean Difference	0	

df	23
t Stat	-2.37233
P(T<=t) one-tail	0.013211
t Critical one-tail	1.31946
P(T<=t) two-tail	0.026421
t Critical two-tail	1.713872

t-Test: Two-Sample Assuming Unequal Variances

Mg	*Erodible*	*Non-erodible*
Mean	1.440329	1.955556
Variance	1.600716	0.653257
Observations	15	15
Hypothesized Mean Difference	0	
df	24	
t Stat	-1.32914	
P(T<=t) one-tail	0.098151	
t Critical one-tail	1.317836	
P(T<=t) two-tail	0.196301	
t Critical two-tail	1.710882	

t-Test: Two-Sample Assuming Equal Variances

N	*Erodible*	*Non-Erodible*
Mean	0.0280747	0.0419328
Variance	8.205E-05	0.000103206
Observations	15	15
Pooled Variance	9.263E-05	
Hypothesized Mean Difference	0	
df	28	
t Stat	-3.9433018	
P(T<=t) one-tail	0.0002446	
t Critical one-tail	1.3125268	
P(T<=t) two-tail	0.0004891	
t Critical two-tail	1.7011309	

t-Test: Two-Sample Assuming Equal Variances

CEC	*Variable 1*	*Variable 2*
Mean	6.6642667	9.754
Variance	2.1498319	2.249482857

Observations	15	15
Pooled Variance	2.1996574	
Hypothesized Mean Difference	0	
df	28	
t Stat	-5.7052425	
P(T<=t) one-tail	2.028E-06	
t Critical one-tail	1.3125268	
P(T<=t) two-tail	4.057E-06	
t Critical two-tail	1.7011309	

t-Test: Two-Sample Assuming Unequal Variances

Ca	*Erodible*	*Non-erodible*
Mean	16.24865	20.53915
Variance	335.7708	90.72142
Observations	15	15
Hypothesized Mean Difference	0	
df	21	
t Stat	-0.80463	
P(T<=t) one-tail	0.215024	
t Critical one-tail	1.323188	
P(T<=t) two-tail	0.430047	
t Critical two-tail	1.720743	

t-Test: Two-Sample Assuming Equal Variances

Al	*Variable 1*	*Variable 2*
Mean	46.97553	54.29808
Variance	413.8876	387.6383
Observations	15	15
Pooled Variance	400.763	
Hypothesized Mean Difference	0	
df	28	
t Stat	-1.00173	
P(T<=t) one-tail	0.162527	
t Critical one-tail	1.312527	
P(T<=t) two-tail	0.325054	
t Critical two-tail	1.701131	

t-Test: Two-Sample Assuming Unequal Variances

Na	*Variable 1*	*Variable 2*
Mean	0.015081	0.019014
Variance	1.65E-05	8.15E-05

Observations	15	15
Hypothesized Mean Difference	0	
df	19	
t Stat	-1.53891	
P(T<=t) one-tail	0.070157	
t Critical one-tail	1.327728	
P(T<=t) two-tail	0.140314	
t Critical two-tail	1.729133	

t-Test: Two-Sample Assuming Equal Variances

Fe	*Variable 1*	*Variable 2*
Mean	34.15219	36.58949
Variance	59.19354	65.33538
Observations	15	15
Pooled Variance	62.26446	
Hypothesized Mean Difference	0	
df	28	
t Stat	-0.8459	
P(T<=t) one-tail	0.20239	
t Critical one-tail	1.312527	
P(T<=t) two-tail	0.404779	
t Critical two-tail	1.701131	

pH

t-Test: Two-Sample Assuming Equal Variances

pH	*Variable 1*	*Variable 2*
Mean	4.846666667	5.196666667
Variance	0.056033333	0.007033333
Observations	3	3
Pooled Variance	0.031533333	
Hypothesized Mean Difference	0	
df	4	
t Stat	-2.41395257	
P(T<=t) one-tail	0.036620346	
t Critical one-tail	1.533206274	
P(T<=t) two-tail	0.073240691	
t Critical two-tail	2.131846786	

t-Test: Two-Sample Assuming Equal Variances

EC

EC	*Variable 1*	*Variable 2*

Mean	0.01	0.013333333
Variance	0	3.33333E-05
Observations	3	3
Pooled Variance	1.66667E-05	
Hypothesized Mean Difference	0	
df	4	
t Stat	-1	
P(T<=t) one-tail	0.186950483	
t Critical one-tail	1.533206274	
P(T<=t) two-tail	0.373900966	
t Critical two-tail	2.131846786	

Correlation matrix P values

	Wet	Dry
%C	0.0225	0.0019
P (mg/kg)	0.0737	0.2522
%N	0.0204	0.0007
K (cmol(+)/kg)	0.0108	0.6315
Ca (cmol(+)/kg)	0.7425	0.1844
Mg (cmol(+)/kg)	0.3603	0.5131
Na (cmol(+)/kg)	0.3257	0.0097
CEC (cmol(+)/kg)	0.0178	0.0001
Al (mg/kg)	0.9128	0.5208
Fe (mg/kg)	0.3243	0.0115

Appendix B: Multi linear regression analysis dry- and wet aggregate stability

Wet stab model

Regression Statistics	
Multiple R	0.623809
R Square	0.389138
Adjusted R Square	0.261875
Standard Error	3.769109
Observations	30

ANOVA

	df	*SS*	*MS*	*F*	*Significance F*
Regression	5	217.1944	43.43889	3.057745	0.028302
Residual	24	340.9484	14.20618		
Total	29	558.1428			

	Coefficients	*Standard Error*	*t Stat*	*P-value*	*Lower 95%*	*Upper 95%*
Intercept	-2.90931	3.911591	-0.74377	0.464238	-10.9824	5.163817
X Variable 1	0.183158	0.614174	0.298218	0.768104	-1.08444	1.45075
X Variable 2	0.0135	0.017029	0.792771	0.435678	-0.02165	0.048647
X Variable 3	0.91951	0.44524	2.065198	0.049867	0.000579	1.838441
X Variable 4	0.418756	0.512886	0.81647	0.422262	-0.63979	1.477301
X Variable 5	0.126994	0.104265	1.217998	0.235064	-0.0882	0.342187

Wet stab model adjusted

Regression Statistics	
Multiple R	0,697247
R Square	0,486153
Adjusted R Square	0,363808
Standard Error	2,110438
Observations	27

ANOVA

	df	*SS*	*MS*	*F*	*Significance F*
Regression	5	88,49188	17,69838	3,973637	0,010797
Residual	21	93,53293	4,453949		
Total	26	182,0248			

	Coefficients	*Standard Error*	*t Stat*	*P-value*	*Lower 95%*	*Upper 95%*
Intercept	2,121042	2,298318	0,922867	0,366559	-2,65857	6,900656
C	0,36853	0,355372	1,037028	0,311517	-0,37051	1,107566
P	0,014724	0,010521	1,399488	0,176265	-0,00716	0,036602
K	0,413048	0,303893	1,359189	0,188505	-0,21893	1,045029
CEC	0,347396	0,299928	1,158264	0,25976	-0,27634	0,971131
FE	-0,02999	0,064192	-0,46712	0,645222	-0,16348	0,103508

Dry stab model

SUMMARY OUTPUT

Regression Statistics	
Multiple R	0.835052
R Square	0.697312
Adjusted R Square	0.648881
Standard Error	2.621945
Observations	30

ANOVA

	df	*SS*	*MS*	*F*	*Significance F*
Regression	4	395.93	98.9825	14.3983	3.16E-06
Residual	25	171.8649	6.874597		
Total	29	567.7949			

	Coefficients	*Standard Error*	*t Stat*	*P-value*	*Lower 95%*	*Upper 95%*
Intercept	-8.30732	2.752541	-3.01805	0.005782	-13.9763	-2.63835
C	1.243019	0.284522	4.368793	0.000191	0.657034	1.829003
Ca	0.068776	0.033581	2.048092	0.051191	-0.00038	0.137937
Na	136.775	75.34014	1.815434	0.081472	-18.3909	291.941
Fe	0.303056	0.06321	4.794456	6.35E-05	0.172874	0.433239

Dry stab model adjusted	
Multiple R	0.776586927
R Square	0.603087255
Adjusted R Square	0.573686311
Standard Error	2.889092104
Observations	30

ANOVA

	df	*SS*	*MS*	*F*	*Significance F*
Regression	2	342.4299	171.2149	20.51251	3.82E-06
Residual	27	225.365	8.346853		
Total	29	567.7949			

	Coefficients	*Standard Error*	*t Stat*	*P-value*	*Lower 95%*	*Upper 95%*
Intercept	-6.093037698	2.902947	-2.09891	0.045312	-12.0494	-0.13668
C	1.469491941	0.283073	5.191208	1.82E-05	0.888674	2.05031
FE	0.317145875	0.069322	4.574967	9.54E-05	0.174909	0.459383

Appendix C: Clay mineralogy

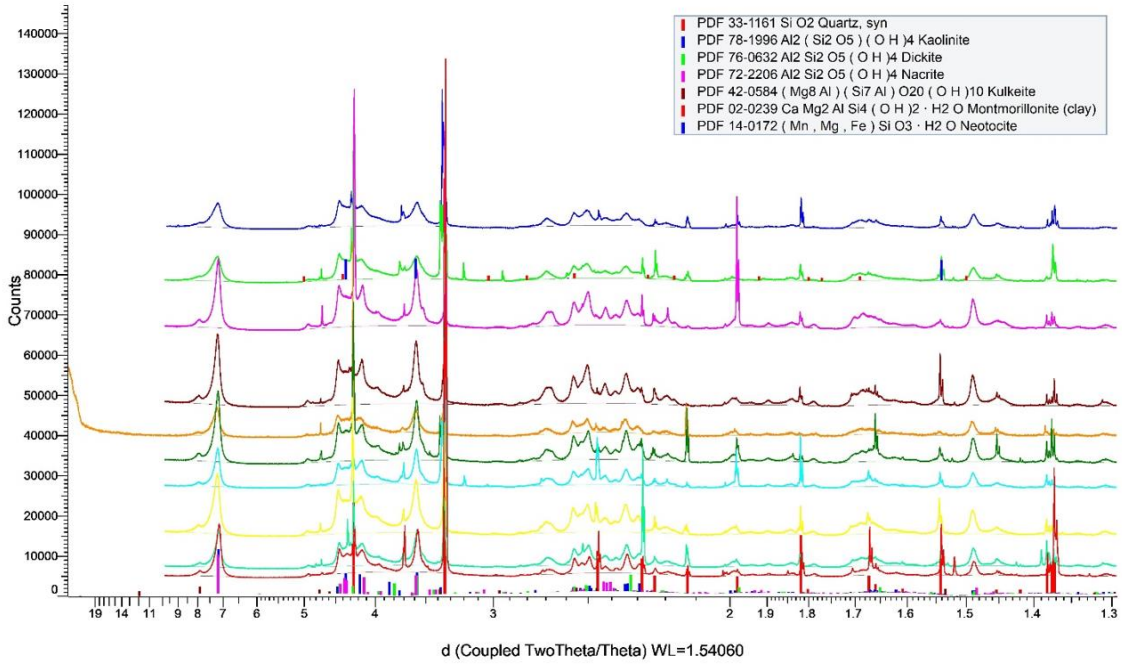

(Coupled TwoTheta/Theta)

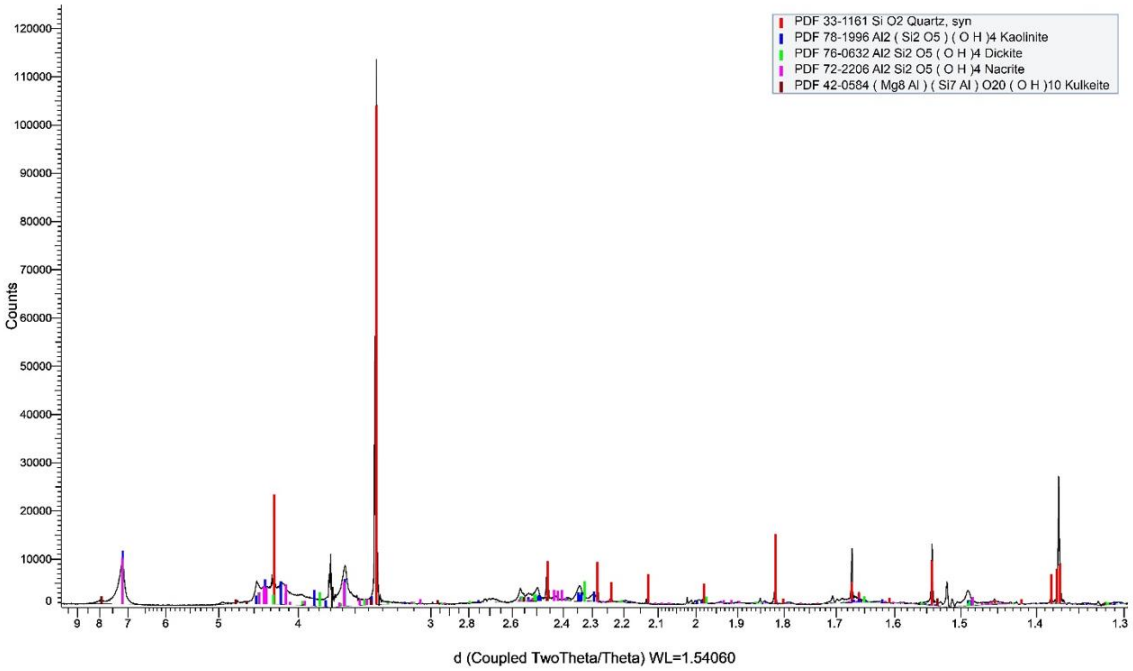

Appendix D: Modelled outcomes

		mm	ton/ha
Agg.Stab	EHD	Runoff	Soil loss
10	0.05	582.26	12.94
20	0.06	545.78	11.74
30	0.07	459.93	9.08
40	0.08	408.77	7.61
50	0.09	363.30	6.38
60	0.1	322.89	5.34
70	0.11	286.97	4.48

Original model	mm	ton/ha
EHD	Runoff	Soil loss
0.05	637.93	14.59
0.06	577.41	12.56
0.07	522.64	10.82
0.08	473.06	9.32
0.09	428.19	8.02
0.1	387.57	6.91
0.11	350.81	5.95